Evaluation of Probabilistic Seismic Hazard Analyses based on macroseismic observations

Work Package #5 "PSHA"

AUTHORS Name	Date	REVIEW Name	Date	APPROVAL Name	Date
Kamel Drif *Pierre Labbé* *Gloria Senfaute*	*2019/05/03*	*Paolo Bazzurro* *Christophe Martin*	*2020/11/09*	Emmanuel Viallet ***Public access*** ◉ ***SIGMA-2 restricted*** ○	2021/08/24

DISSEMINATION: *This document must not be distributed to any person, institution or company other than members of SIGMA-2 steering and scientific committees, except under written formal permission of SIGMA-2 steering committee.*

Document history

DATE	VERSION	COMMENTS
2018/09/10	*1*	*Draft version for Scientific Committee review*
2019/05/03	*1*	*Final version*

Table of contents

1 Introduction

Probabilistic seismic hazard analysis (PSHA) has become a fundamental tool in assessing seismic hazards and seismic input motions. It is used for both site-specific evaluation in case of critical facilities and at national or regional scale for building codes.

PSHA outcomes are expected to be affected by uncertainty due to imperfect knowledge of physical processes that generate the seismic ground shaking (faulting, seismic wave propagation, etc.), This uncertainty (being large or small) is an important component of PSHA outcomes and implies that several possible situations (seismic scenarios) may occur during the expected operational period (TecDoc IAEA in progress). Considering this high uncertainty in Probabilistic Seismic Hazard Assessments (PSHA) and the importance of PSHA for the seismic design, it is largely pertinent to focus on the issue of consistency-checking of the PSHA outcomes.

PSHA outcomes can be evaluated against different types of observations, such as accelerations recorded at instrumented sites (Stirling et al. 2010, Fujiwara et al. 2009, Albarello et al. 2008, Viallet et al. 2008), macroseismic intensities (Stirling et al. 2006), or maximum acceleration levels based on precarious fragile structures (Brune et al. 2002). Methods to compare probabilistic estimates with observations range from purely qualitative techniques to quantitative statistical methods. They either focus on sites (a specific site or a set of several sites) or embrace a regional scale area. The approach presented in this report is of this latter type.

In recent years, increasing efforts have been devoted to assessing the reliability of PSHA results, different kinds of procedures have been tested and many papers have provided useful information on this topic. In 2015, the OECD Nuclear Energy Agency, in cooperation with the IAEA, organized a workshop hosted by EUCETER (Pavia University) on Testing Probabilistic Seismic Hazard Analysis Results and the Benefits of Bayesian Techniques (OECD/NEA 2015). The main recommendation issued by this workshop was: *A state-of-the-art PSHA should include a testing phase against any available observation, including any kind of observation and any period of observation, including instrumental seismicity, historical seismicity and paleoseismicity data if available. It should include testing not only against its median hazard estimates but also against their entire distribution (percentiles)*.

In the last decade, several approaches for testing PSHA results have been published. Several recent opinion papers encourage hazard analysis to carry out tests (Stein 2011, Stirling 2012) and several applications have been made in different countries (France, Italy, New Zealand, USA, Mexico, etc) (Stirling et al. 2006, Brune et al. 2002, Rey et al. 2018). For evaluating PSHA outcomes against observations, most researches use accelerations recorded at instrumented sites. However, stable continental regions with low deformation rates and low seismicity have not sufficient seismic activity (the level of accelerations is too low) or the period of observations is too short for testing PSHA outcomes. For these regions, the use of macroseismic data is of primary interest when dealing with seismic hazard analysis and particularly for testing the consistency of seismic hazard estimates with observations.

However, despite this interest, researches on the subject are not too much developed. The objective of the present research is to apply a method based on macroseismic data (Labbé 2008, 2010, 2017), so as to evaluate the consistency with historical seismicity of three hazard maps of the French metropolitan territory (established in 2002, 2012 and 2017), which reveal a dramatic lack of consensus on the subject. For practical reasons, the consistency evaluation is limited to the continental France.

The method does not consist of directly comparing accelerations with intensities, but of calculating the seismic risk by two different approaches presented in section 2. The seismic risk is defined as the annual probability that a building of a given vulnerability class experiences a given damage grade, where the vulnerability class and the damage grade are defined in the EMS-98 scale (Grünthal 1998).

Editorial remark: In this report the term “continental France” means “metropolitan French territory, Corsica excluded”.

2 Methodological approach

The methodology applied in this research consists in calculating the seismic risk using two different approaches (Labbé 2008, 2010, 2017):

1) Seismic risk 1, derived from historical seismicity.
2) Seismic risk 2, calculated by convolution of hazard maps and fragility curves.

The seismic risk derived from historical seismicity (macroseismic observations) is considered as the “reference” for comparing with the seismic risk obtained by convolution.

Next paragraphs are describing the principle of calculation of both methods explored in this research.

2.1 Seismic risk derived from historical seismicity

2.1.1 Seismic hazard derived from historical seismicity

The calculation of seismic hazard based on historical seismicity considers the ratio between the annual average area affected by an intensity equal to or larger than I in a region of interest and the total area of this region.

2.1.1.1 Principle of calculation

We consider a territory of area A, inside which the seismic activity is deemed to be homogeneous (in space) and stationary (in time). We denote A_I the average area of this territory yearly affected by an intensity equal to or larger than I. Then the annual observing frequency (I) of at least one intensity equal to or larger than I at any location in the territory reads:

$$p(I) = \mathrm{A}_I \,/\, \mathrm{A}. \qquad (1)$$

Conceptually, would we have at our disposal comprehensive macro-seismic data on a very long period of time (T years), calculating A_I would be easily achieved as follows: For every event i occurring during the period of time T, we denote $\mathcal{A}_{\mathrm{i},I}$ the area affected by an intensity larger than or equal to I. Then

$$\mathrm{A}_I = \mathcal{A}_I / \mathrm{T} \quad \text{with} \quad \mathcal{A}_I = \Sigma\, \mathcal{A}_{\mathrm{i},I} \qquad (2)$$

2.1.1.2 Practical implementation

Practical implementation of the above approach faces two difficulties. The first one is that we do not have at our disposal the above-mentioned ideal comprehensive information. However, considering the Continental France, we have, in MSK scale, a comprehensive set of isoseismals of those earthquakes felt in the territory in the years 1900-2007 (T=108 y), whose epicentral intensities are equal to or larger than VI (Pecker et al 2017). This enables us to derive, for I>=VI, an estimated value, $p'(I)$, of $p(I)$ as follows:

$$p'(I) = \mathrm{A}'_I \, / \, \mathrm{A}. \qquad (1')$$

$$\mathrm{A}'_I = \mathcal{A}'_I/108 \quad \text{with } \mathcal{A}'_I = \Sigma\, \mathcal{A}_{\mathrm{i},I} \text{ on 1900-2007} \qquad (2')$$

The second difficulty is that the Continental France cannot be regarded as homogeneous in terms of seismic activity. In order to address this variability, we separate the territory into 8 domains, presented further, in such a way that the activity can be regarded as reasonably homogeneous inside a domain.

Consequences of these two difficulties are addressed in section 3.1.

2.1.2 Transition to historically observed seismic risk

2.1.2.1 Relevant features of the EMS-98 scale

Consistently with the MSK scale used in Lambert et al 2015, the EMS-98 scale (Grünthal 1998) is selected to derive the seismic risk from the historical seismic hazard. The EMS-98 scale is based on:

- **Differentiation of buildings into vulnerability classes**

Four types of structures are differentiated namely: masonry, reinforced concrete, steel and wood. Figure 1, copied from the EMS-98 scale for masonry, presents the classification into vulnerability classes $C = \mathrm{A}, \ldots, \mathrm{F}$, where A is the class of the most vulnerable buildings and F the class of the most resistant ones.

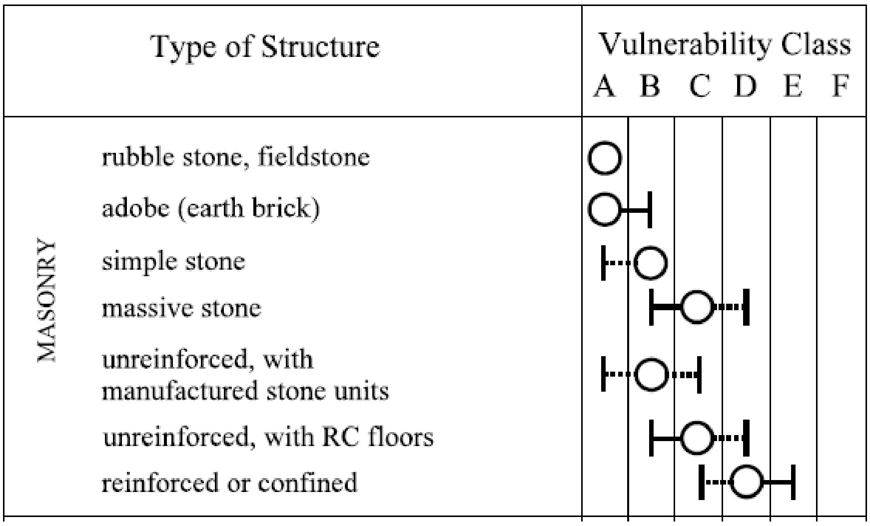

Figure 1 : Classification of vulnerability classes for masonry, scale EMS-98 (Grünthal 1998)

- **Classification of damages**

Five grades of damage are considered, whose definitions are depending on the type of structure. Definitions for masonry are presented in Figure 2.

Classification of damage to masonry buildings	
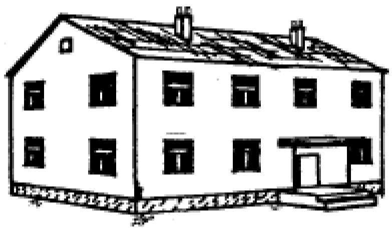	**Grade 1: Negligible to slight damage** **(no structural damage,** **slight non-structural damage)** Hair-line cracks in very few walls. Fall of small pieces of plaster only. Fall of loose stones from upper parts of buildings in very few cases.
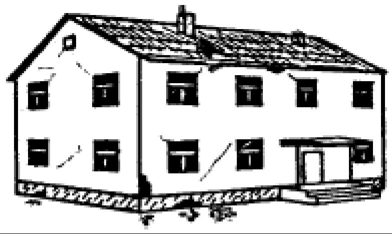	**Grade 2: Moderate damage** **(slight structural damage, moderate non-structural damage)** Cracks in many walls. Fall of fairly large pieces of plaster. Partial collapse of chimneys.
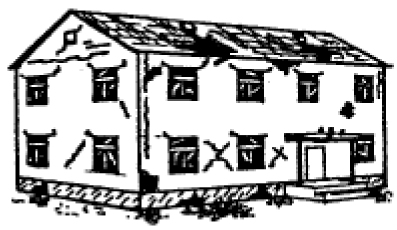	**Grade 3: Substantial to heavy damage** **(moderate structural damage,** **heavy non-structural damage)** Large and extensive cracks in most walls. Roof tiles detach. Chimneys fracture at the roof line; failure of individual non-structural elements (partitions, gable walls).
	**Grade 4: Very heavy damage** **(heavy structural damage,** **very heavy non-structural damage)** Serious failure of walls; partial structural failure of roofs and floors.
	**Grade 5: Destruction** **(very heavy structural damage)** Total or near total collapse.

Figure 2: Classification of masonry damage degrees following the scale EMS-98.

- **Definition of quantity**

The EMS-98 scale quantifies the qualitative words "most", "many" and "few" through a scheme reported in Figure 3.

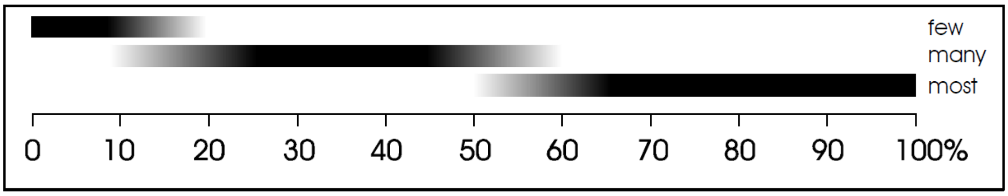

Figure 3: Quantitative interpretation of the qualitative terms as presented in the EMS-98 Scale

The final quantification retained for this study is: most = 80%, many = 35% and few = 8%. The qualification “all” is a probability of 100%.

- **Definition of intensity degrees**

Intensity degree definition considers effects on humans, effects on objects and on nature, and damage to buildings. In the framework of the present study, we focus on damage to buildings. Excerpts of intensity definitions that pertain to this study are:

- Intensity V:

Damage of grade 1 to a few buildings of vulnerability class A and B.

- Intensity VI:

Damage of grade 1 is sustained by many buildings of vulnerability class A and B; a few of class A and B suffer damage of grade 2; a few of class C suffer damage of grade 1.

- Intensity VII:

Many buildings of vulnerability class A suffer damage of grade 3; a few of grade 4. Many buildings of vulnerability class B suffer damage of grade 2; a few of grade 3. A few buildings of vulnerability class C sustain damage of grade 2. A few buildings of vulnerability class D sustain damage of grade 1.

- Intensity VIII:

Many buildings of vulnerability class A suffer damage of grade 4; a few of grade 5. Many buildings of vulnerability class B suffer damage of grade 3; a few of grade 4. Many buildings of vulnerability class C suffer damage of grade 2; a few of grade 3. A few buildings of vulnerability class D sustain damage of grade 2.

- Intensity IX:

Many buildings of vulnerability class A sustain damage of grade 5. Many buildings of vulnerability class B suffer damage of grade 4; a few of grade 5. Many buildings of vulnerability class C suffer damage of grade 3; a few of grade 4. Many buildings of vulnerability class D suffer damage of grade 2; a few of grade 3. A few buildings of vulnerability class E sustain damage of grade 2.

These effects on buildings are summarized in the Table 1. Terms in green are not explicitly mentioned in the EMS-98 scale. They are the result of an interpretation of the scale by the authors, in the continuity of terms that are explicitly mentioned (in blue).

Intensité V

	Vulnerability classes				
degrees of damage	A	B	C	D	E
1	few	few	-	-	-
2	-	-	-	-	-
3	-	-	-	-	-
4	-	-	-	-	-
5	-	-	-	-	-

Intensité VI

	Vulnerability classes				
degrees of damage	A	B	C	D	E
1	many	many	few	-	-
2	few	few	-	-	-
3	-	-	-	-	-
4	-	-	-	-	-
5	-	-	-	-	-

Intensité VII

	Vulnerability classes				
degrees of damage	A	B	C	D	E
1	all	most	many	few	-
2	most	many	few	-	-
3	many	few	-	-	-
4	few	-	-	-	-
5	-	-	-	-	-

Intensité VIII

	Vulnerability classes				
degrees of damage	A	B	C	D	E
1	all	all	most	many	-
2	all	most	many	few	-
3	most	many	few	-	-
4	many	few	-	-	-
5	few	-	-	-	-

Intensité IX

	Vulnerability classes				
degrees of damage	A	B	C	D	E
1	all	all	all	most	many
2	all	all	most	many	few
3	all	most	many	few	-
4	most	many	few	-	-
5	many	few	-	-	-

Table 1: Transition from the seismic hazard in intensity to damage to buildings. In blue, terms that are explicitly used in EMS-98, in green interpretation by the authors.

2.1.2.2 *Risk calculation*

Combining the definition of intensity and quantity, we introduce $F_D^C(I)$, probability that a damage D or larger than D occurs in a building of vulnerability class C in case an intensity I is observed or assumed. Values of $F_D^C(I)$ result from the Table 1, replacing the qualitative terms by their quantified values.

Eventually, once the seismic hazard is described in terms of intensities, it is possible to calculate the seismic risk, $R^C(D)$, already introduced as the annual probability that a building of vulnerability class C experiences a damage D, by:

$$R^C(D) = \sum_{I=VI}^{IX} p(I)\, F_D^C(I) \qquad (3)$$

Because we do not have a comprehensive information on Intensity V, the summation starts at I=VI. Consequently, the above formula (3) is only valid for D>1.

Remark: In this approach, it is necessary that the seismic hazard is described in terms of intensities, but it is not necessary that this description is derived from historical seismicity in the way presented in 2.1.1.

2.2 Principle of calculation of seismic risk based on probabilistic seismic hazard models and fragility curves

It is assumed here that probabilistic seismic hazard models provide values in acceleration (PGA, Peak Ground Acceleration) and that concurrently fragility curves in PGA are available for at least some classes of vulnerability. Under these conditions, the seismic risk $R^{C}(D)$ in a location inside the territory can be calculated by the convolution integral:

$$R^{C}(D) = \int_{0}^{\infty} -H'(a)\, F_{D}^{C}(a) da \tag{4}$$

where:

$H\,(a)$ is the seismic hazard or annual frequency of observing a PGA equal or greater than a at the considered location.

$F_{D}^{C}(a)$ is the fragility curve or probability that the acceleration inducing a damage of degree D in a building of vulnerability class C is lower than a.

An analytical expression of the above integral is available under two conditions:

- The hazard curve is replaced by its tangent line at the point corresponding to a defined return period, T_{ref}, as illustrated in Figure 4-a.
- Building fragilities are log normally distributed, as illustrated in Figure 4-b.

On these bases, the above integral (4) takes the value given by the formula (5). Formula (4) and (5) were proposed, established and used for instance by Kennedy (1999).

$$R^{C}(D) = \int_{0}^{\infty} -H'\,(a)\, F_{D}^{C}(a)da \approx \frac{1}{T_{ref}} \left(\frac{a_{ref}}{a_{D}^{C}}\right)^{n} exp\left(\frac{n^{2} {\beta_{D}^{C}}^{2}}{2}\right) \tag{5}$$

where:

T_{ref} : return period selected for establishing the probabilistic seismic hazard analysis,

a_{ref}: PGA at the considered T_{ref} ,

a_{D}^{C} : median value of PGAs generating a damage grade D in a building of vulnerability class C,

β_{D}^{C}: standard deviation of the logarithm of the PGAs generating a damage grade D in a building of vulnerability class C,

n : slope in log-log scale at a_{ref} of the line tangent to the seismic hazard curve at the considered location.

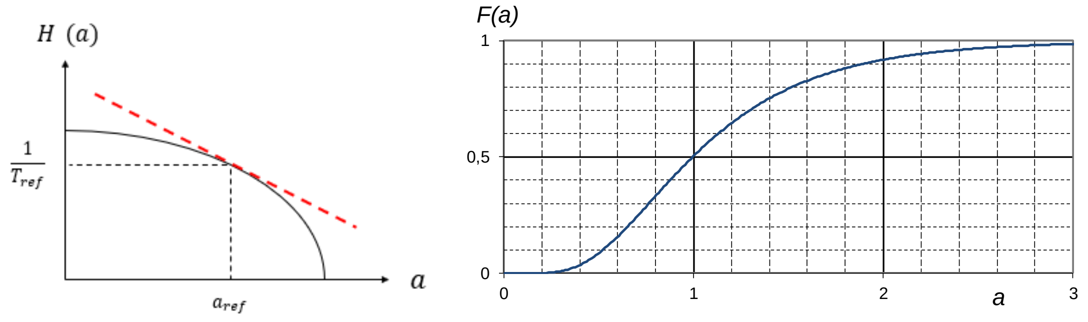

Figure 4: Scheme of seismic hazard curve, parameters T_{ref} and a_{ref}, and tangent line at a_{ref}. (left) and typical lognormal fragility curve plotted for median PGA =1 and β=0.5 (right)

3 Application to the continental France

3.1 Seismic risk derived from historical seismicity

3.1.1 Description of input data

An atlas of isoseismal maps was elaborated in the framework of the SIGMA research development project (Senfaute et al. 2015, Pecker et al. 2017). This atlas (identified as "the SIGMA atlas" in the following) comprises earthquakes drawn from the SisFrance database (http://www.sisfrance.net/). The SIGMA atlas is an exhaustive set of manually drawn isoseismals for events with epicentral intensities of degree VI (MSK) or greater, occurring over the period 1900 to 2007, and felt in continental France or its immediate vicinity (194 events), Lambert 2015. Details on these 194 events are presented in the Annex 4.

Even if some manual isoseismal drawing were already available for some of the events of interest (Levret et al. 1994), this new atlas provides a homogeneous dataset of isoseismals based on a unique approach and with drawing associated to reliability indexes. Figure 5 illustrates the location of the 194 epicentres under consideration. Figure 6 presents an example of isoseismal map derived from the Intensity Data Points (IDPs)

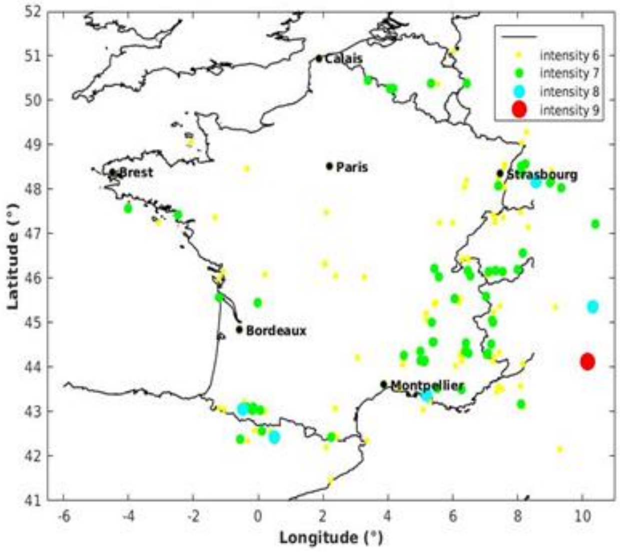

Figure 5: Location of epicentres with intensity equal to or greater than VI over the period 1900 – 2007

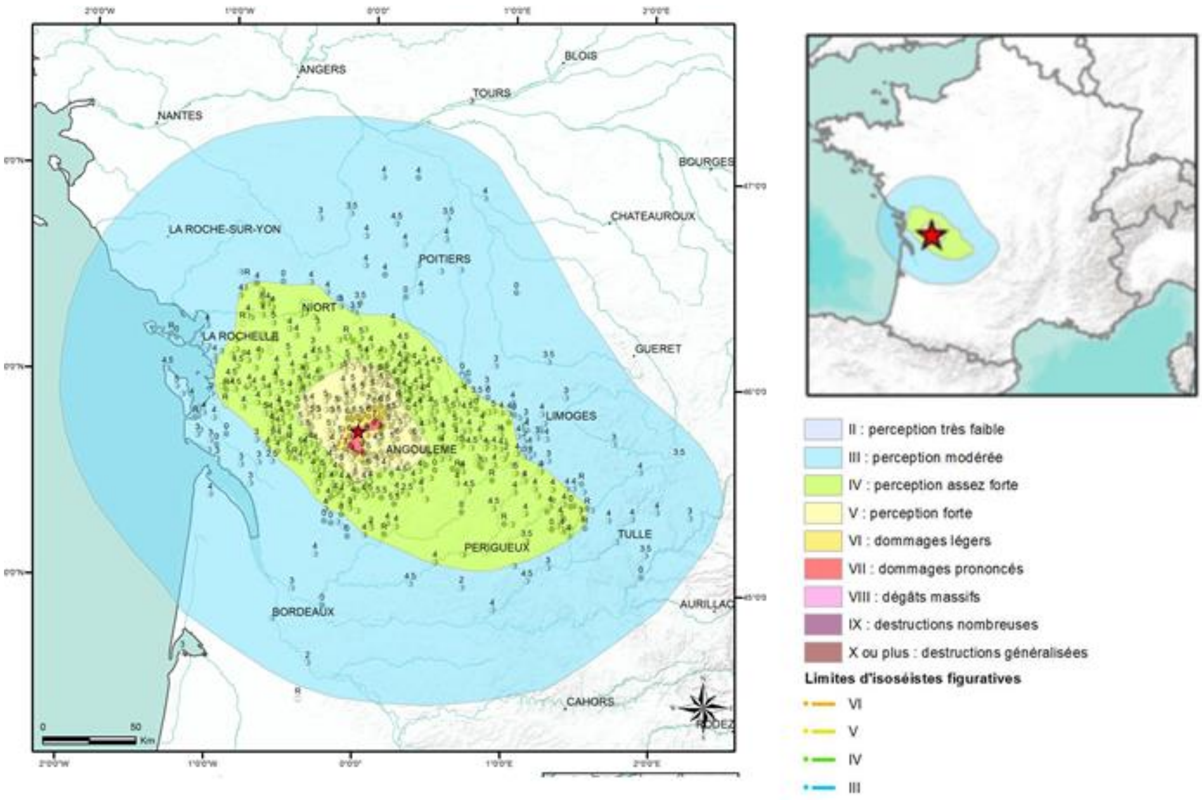

Figure 6: Example of isoseismal map derived from the Intensity Data Points. The intensity of the epicentre was evaluated at VII (Lambert et al. 2015).

Continental France is a moderate seismicity area. The activity is usually diffuse and not homogeneous across the territory. In order to identify reasonably homogeneous domains, we rely on seismo-tectonic studies that were conducted by Drouet et al. 2017 to individualize crustal units of homogenous seismogenic characteristics, on the basis of criteria related to static and dynamic state of the seismogenic crust (geometry and kinematic of tectonic structures, distribution of seismicity activity, stress field...). These deemed homogeneous domains are presented in Figure 7. Domain areas (in km²) are reported in the Table 2, including area of the continental France.

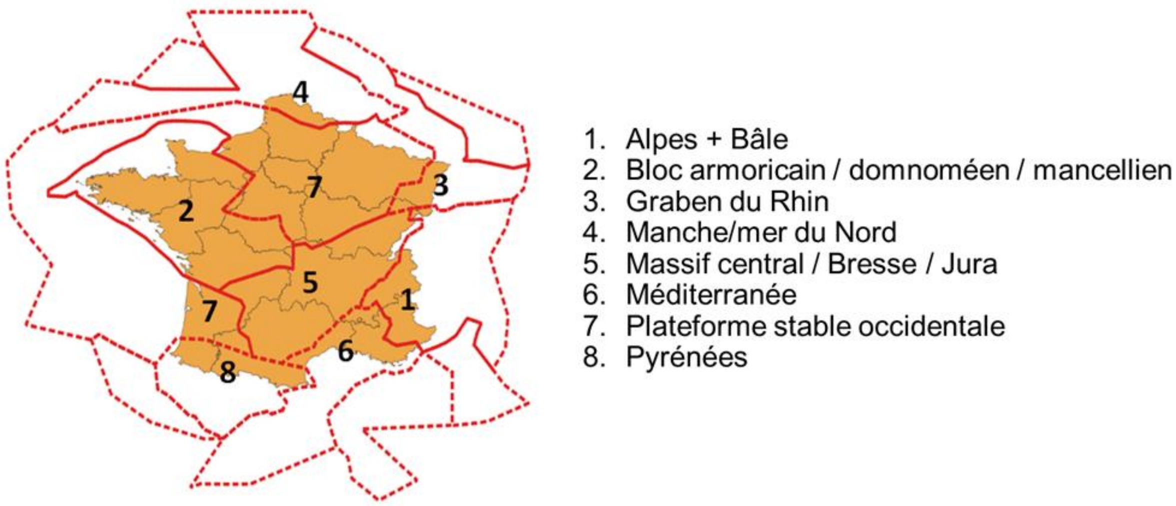

Figure 7: Seismo-tectonic domains relatively homogenous across the French territory.

3.1.2 Completeness and extreme historical events

We may note, for instance, that no Intensity VIII was observed on 1900-2007 in the Alpes-Bâle domain. Obviously, it does not mean that such intensities are not possible. Similarly, no intensity 9 was observed in the continental France, which does not mean it could never happen. This raises the issue of the consequences of the lack of completeness of only one century of observations, which issue can be split into two questions to be resolved:

- Question 1: To what extent the seismic hazard estimates such as presented in Table 3 could be affected by the considering extreme events that are not in the 1900-2007 data base?
- Question 2: How can we introduce in the hazard assessment the fact that events stronger than those observed in the period 1900-2007 could occur?

Answer to question 1 is founded on:

a) A statistical analysis of isoseismal radii of our data base, presented in the Annex 4. A remarkable output is that, for an epicentral intensity I_0, radii of isoseismals $I \leq I_0$ are log-normally distributed with an excellent coefficient of determination.
b) The analysis of extreme events presented in the Annex 5. These events, which occurred in the 16th, 17th and 18th centuries are extreme in the sense that, for their epicentral intensities, the extension of isoseismals are much larger than observed in our database. In Annex 5, we discuss whether, on the basis of the 1900-2007 statistics,

these large values can be regarded as the expected extreme values on a period of time of 2, 3 or 4 centuries.

From the analyses carried out in Annexes 4 and 5, it results that the historically observed extreme events are representative of the statistically expected extreme events in the considered period of time. Would series of 2, 3 or 4 centuries of historical seismicity be simulated on the basis of the 1900-2007 statistics, such events would likely appear in the series. Consequently, it can be concluded that the hazard assessment carried out on the basis of the 1900-2007 database is not to be corrected in the light of extreme events that are not in the database.

As concerns the question 2: the frequencies calculated for high intensities are null. It means that no isoseismal of these intensities has been observed during the 1900-2007 period. It does not mean that an event of high intensity could not occur. In order to avoid the null frequencies, the high intensity frequencies must be calculated not directly based on observed isoseismals of SISFRANCE database. There are several possibilities. The simplest possibility is to estimate frequencies of high intensities by extending the hazard curves towards the high intensities. Another possibility would be to use the extreme value theory (EVT) to estimate the distribution of high intensities frequencies as Dutfoy (2018) made it for extreme magnitude values. Furthermore, the estimation of extreme frequencies could be obtained by generating a number of extreme earthquakes from a Gutenberg-Richter law and estimate the isoseismal areas affected by these earthquakes using for example a distribution of the isoseismal radii as in Labbé (2018). However, for the latter possibility it would be necessary on the one hand to generate French earthquakes but also abroad ones that could have an impact on the France territory. On the other hand, the spatial distribution of these generated earthquakes must be known in order to affect the French part of these generated isoseismals to the right domain if the hazard is assessed by domain such as the figure 7.

This study uses the first possibility and the hazard curves presented in table 3 are extended towards high frequencies.

3.1.3 Seismic hazard estimate

In order to apply the method described in section 2.1, we first need to calculate the distribution of isoseismal areas in the 8 identified domains. For this purpose, we have plotted all the isoseismals of the considered 194 events of the SIGMA atlas, as presented in Figure 8, and used the QGIS software to calculate the total area affected by the intensity I, in each domain. These areas, as well as the domain areas, are summarized in the Table 2.

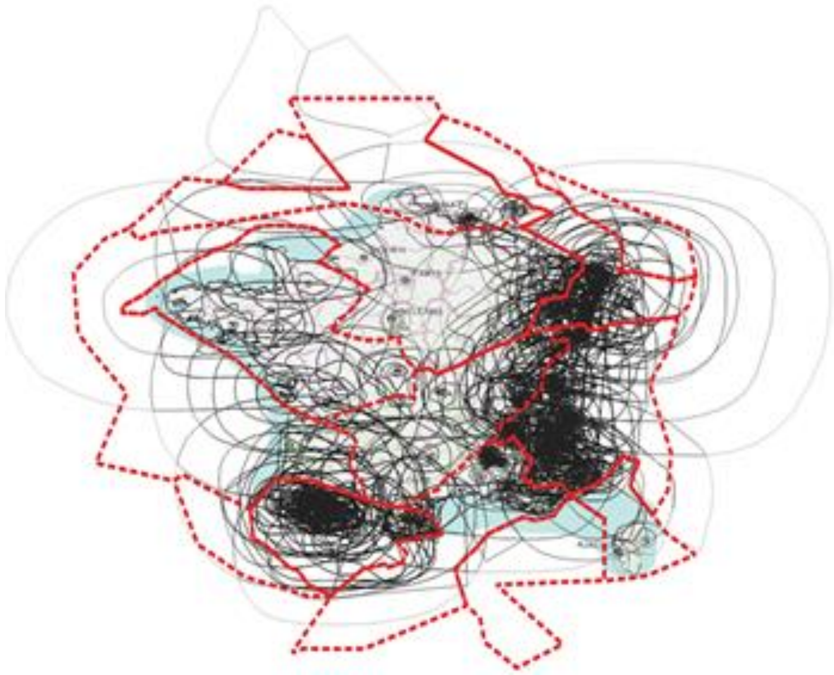

Figure 8: Superposition of isoseists of all epicentres of intensity ≥ VI during the 1900-2007 period

DOMAINS \ INTENSITIES (MSK)	VI	VII	VIII	IX	DOMAIN AREA
ALPES + BALE	10693.02	1731.13	*338.69*	*66.26*	30591.00
BLOC ARMORICAIN / DOMNOMEEN / MANCELLIEN	3140.99	396.45	*50.04*	*6.32*	125670.84
GRABEN DU RHIN	1133.52	6.68	*0.04*	*0.00*	12487.58
MANCHE / MER DU NORD	442.66	10.17	*0.23*	*0.01*	8623.73
MASSIF CENTRAL / BRESSE / JURA	878.47	17.67	*0.36*	*0.01*	124008.54
MEDITERRANEE	2830.22	565.31	210.90	*78.68*	41153.39
PLATEFORME STABLE OCCIDENTALE	84.07	*1.69*	*0.03*	*0.00*	175088.54
PYRENEES	14367.93	1470.03	26.78	*0.49*	29929.19
CONTINENTAL FRANCE	33570.89	4197.43	627.07	151.76	547552.81

Table 2: Areas affected during the 1900-2007 period by an intensity I or higher (I=VI, VII, VIII) in each domain, and domain areas (km²). The values in italic are not directly derived from observed isoseismals (because of the lack of information cf. paragraph 3.1.2)

Applying the equation 1', we calculate for every domain an estimate of the seismic hazard based on historical seismicity. The result of this calculation is presented in the Table 3. In most domains, the fact that no intensity VIII and IX was observed between 1900 and 2007 results in a zero estimated probability.

DOMAINS \ INTENSITIES (MSK)	VI	VII	VIII	IX
ALPES + BALE	3.24E-03	5.24E-04	*1.03E-04*	*2.01E-05*
BLOC ARMORICAIN / DOMNOMEEN / MANCELLIEN	2.31E-04	2.92E-05	*3.69E-06*	*4.65E-07*
GRABEN DU RHIN	8.40E-04	4.95E-06	*2.92E-08*	*1.72E-10*
MANCHE / MER DU NORD	4.75E-04	1.09E-05	*2.51E-07*	*5.76E-09*
MASSIF CENTRAL / BRESSE / JURA	6.56E-05	1.32E-06	*2.65E-08*	*5.33E-10*
MEDITERRANEE	6.37E-04	1.27E-04	4.75E-05	*1.77E-05*
PLATEFORME STABLE OCCIDENTALE	4.45E-06	*8.94E-08*	*1.80E-09*	*3.62E-11*
PYRENEES	4.45E-03	4.55E-04	8.28E-06	*1.51E-07*
CONTINENTAL FRANCE	**5.68E-04**	**7.10E-05**	**1.06E-05**	**2.57E-06**

Table 3: Seismic hazard estimate based on historical seismicity in each domain. The values in italic are not directed derived from observed isoseismals (because of the lack of information cf. paragraph 3.1.2).

3.1.3.1 Risk assessment

The section 2.1.2 describes the method for calculating the seismic risk by combining the seismic hazard expressed in Intensity and the EMS-98 scale.

The annual probability of suffering a damage of degree D or higher (D = 2 to 5) for a building of vulnerability class C (C =A to D) is calculated in each domain by formula (3). The table 5 shows the results for each domain and for the continental France.

	ALPES + BALE				BLOC ARMORICAIN / DOMNOMEEN / MANCELLIEN			
Degrees EMS98	A	B	C	D	A	B	C	D
1	3,58E-03	3,07E-03	5,26E-04	9,22E-05	3,63E-04	3,34E-04	3,16E-05	3,96E-06
2	9,48E-04	5,26E-04	9,22E-05	1,52E-05	5,53E-05	3,16E-05	3,96E-06	4,58E-07
3	3,17E-04	9,22E-05	1,52E-05	1,60E-06	1,57E-05	3,96E-06	4,58E-07	3,72E-08
4	9,06E-05	1,52E-05	1,60E-06	0,00E+00	3,92E-06	4,58E-07	3,72E-08	0,00E+00
5	1,36E-05	1,60E-06	0,00E+00	0,00E+00	4,21E-07	3,72E-08	0,00E+00	0,00E+00

	GRABEN DU RHIN				MANCHE / MER DU NORD			
Degrees EMS98	A	B	C	D	A	B	C	D
1	2,38E-03	2,38E-03	6,90E-05	4,06E-07	7,11E-04	7,00E-04	4,20E-05	9,65E-07
2	7,30E-05	6,90E-05	4,06E-07	2,39E-09	5,08E-05	4,20E-05	9,65E-07	2,21E-08
3	2,15E-06	4,06E-07	2,39E-09	1,37E-11	4,90E-06	9,65E-07	2,21E-08	4,61E-10
4	4,06E-07	2,39E-09	1,37E-11	0,00E+00	9,65E-07	2,21E-08	4,61E-10	0,00E+00
5	2,38E-09	1,37E-11	0,00E+00	0,00E+00	2,16E-08	4,61E-10	0,00E+00	0,00E+00

	MASSIF CENTRAL / BRESSE / JURA				MEDITERRANEE			
Degrees EMS98	A	B	C	D	A	B	C	D
1	2,14E-04	2,12E-04	5,73E-06	1,15E-07	9,52E-04	8,44E-04	1,38E-04	3,95E-05
2	6,79E-06	5,73E-06	1,15E-07	2,31E-09	2,34E-04	1,38E-04	3,95E-05	9,99E-06
3	5,89E-07	1,15E-07	2,31E-09	4,27E-11	1,01E-04	3,95E-05	9,99E-06	1,42E-06
4	1,15E-07	2,31E-09	4,27E-11	0,00E+00	3,81E-05	9,99E-06	1,42E-06	0,00E+00
5	2,27E-09	4,27E-11	0,00E+00	0,00E+00	8,58E-06	1,42E-06	0,00E+00	0,00E+00

	PLATEFORME STABLE OCCIDENTALE				PYRENNEES			
Degrees EMS98	A	B	C	D	A	B	C	D
1	1,98E-05	1,97E-05	3,88E-07	7,81E-09	4,78E-03	4,33E-03	5,21E-04	3,94E-05
2	4,60E-07	3,88E-07	7,81E-09	1,56E-10	8,86E-04	5,21E-04	3,94E-05	7,16E-07
3	3,99E-08	7,81E-09	1,56E-10	2,89E-12	2,02E-04	3,94E-05	7,16E-07	1,21E-08
4	7,80E-09	1,56E-10	2,89E-12	0,00E+00	3,94E-05	7,16E-07	1,21E-08	0,00E+00
5	1,54E-10	2,89E-12	0,00E+00	0,00E+00	7,03E-07	1,21E-08	0,00E+00	0,00E+00

	CONTINENTAL FRANCE			
Degrees EMS98	A	B	C	D
1	7,36E-04	6,68E-04	7,92E-05	1,12E-05
2	1,36E-04	7,92E-05	1,12E-05	1,75E-06
3	4,03E-05	1,12E-05	1,75E-06	2,05E-07
4	1,10E-05	1,75E-06	2,05E-07	0,00E+00
5	1,54E-06	2,05E-07	0,00E+00	0,00E+00

Table 5: Seismic risk evaluation on the bases of historical seismicity for four degrees of damage and four classes of vulnerabilities (A, B, C, D) within each domain

3.2 Seismic risk based on Probabilistic Seismic hazard models and fragility curves

3.2.1 Description of input data

Probabilistic seismic hazard models

In the last years, several probabilistic seismic hazard maps have been established for the French territory. The main characteristic of these maps regards the huge variability in the hazard assessment. For the present study three probabilistic seismic hazard maps were selected:

1) MEDD: French probabilistic seismic hazard map established in 2002. This hazard map was used by French organisations to elaborate the French zoning map dividing the country into five levels of hazard. There is not a scientific publication for this hazard map.
2) SHARE: European probabilistic hazard map established in 2013. SHARE was elaborated under the Seventh Framework Program of the European Commission and provide seismic hazard estimates for the Euro-Mediterranean regions (http://www.share-eu.org/).
3) GEOTER: French probabilistic hazard map established in 2017. It is the most recent hazard map of the French metropolitan territory, which integrates the last state of the art and particularly all scientific progress of SIGMA research program (Drouet et al. 2015, Martin et al. 2017). The main progress introduced in GEOTER model are: a new French seismic catalogue, homogenous in moment magnitude, attenuation ground motion models better adapted to the French territory, improved methodologies for a better determination of maximum magnitudes, propagation of uncertainties, etc. Publication of this hazard map is in progress.

Fragility curves

According to the method described in 2.2, it is necessary to know the parameters characterizing the fragility curve namely a_D and β_D (see equation 5). To obtain these parameters, the approach of Lagomarsino & Cattari 2014 is used.

The table 6 indicates the values of a_D and β_D using the conversion formulas intensity to PGA by Murphy & O'Brien 1997, and Faccioli & Cauzzi 2006 for three damage degrees (D2, D3 and D4) and two vulnerability classes (B and C). Annex 1 presents a synthesis of the method to derive the values of table 6.

Vulnerabily class B	D2		D3		D4	
	α_D $[cm.s^{-1}]$	β_D	α_D $[cm.s^{-1}]$	β_D	α_D $[cm.s^{-1}]$	β_D
MURPHY & O'BRIEN (1977)	115,76	0.62	200,12	0.61	348,26	0.63
FACCIOLI & CAUZZI (2006)	142,25	0.54	235,44	0.54	382,59	0.56

Vulnerabilty class C	D2		D3		D4	
	α_D $[cm.s^{-1}]$	β_D	α_D $[cm.s^{-1}]$	β_D	α_D $[cm.s^{-1}]$	β_D
MURPHY & O'BRIEN (1977)	203.99	0.62	355.26	0.61	618.99	0.63
FACCIOLI & CAUZZI (2006)	237.99	0.54	389.52	0.54	637.76	0.56

Table 6: Median values and standard deviation of natural logarithm of PGAs for two conversion formulas, three damages degrees (D2, D3, D4) and two vulnerability classes B and C

A concern with this approach is that the considered fragility curves are derived from intensity observations and conversion formula. In the spirit of our study, another option would be that we use fragility curves that are directly established in terms of PGA, such as those proposed by Milutinovic & Trendafiloski (2003) or Rota et al. (2008). Vulnerability classes to be associated to these fragility curves are not specified by the authors. Regarding Rota et al., the building description is clearly in favour of class C. As Milutinovic & Trendafiloski values are similar, it is also assumed that they are for class C as well.

In any case, it should be observed that, either or not derived from observations in intensity, the available fragility curves take the form of lognormal functions. It means that the intensity intermediate is not a real concern to the extent its effects on seismic risk assessment can be covered by a sensitivity analysis such as presented in Annex 6. For instance, for the damage grade 2, there is a difference of one order of magnitude between the probability derived from the fragility curve of Lagomarsino & Cattari (2014) based on Murphy & O'Brien (1977) and the probability derived from the fragility curve of Rota et al. (2008).

3.2.2 Calculations and results

The seismic risk was derived from each hazard maps (MEDD, SHARE, GEOTER) and each fragility curves described in the precedent chapter, which results in 6 combinations. The seismic risk calculations were done for a grid of 115 points, presented in Figure 10, whose coordinates are listed in the Annex 3.

The risk was calculated at every point by formula (5). The selected T_{ref} is 475 years and the corresponding values of a_{ref} and n are listed in the Annex 3 for the 3 maps.

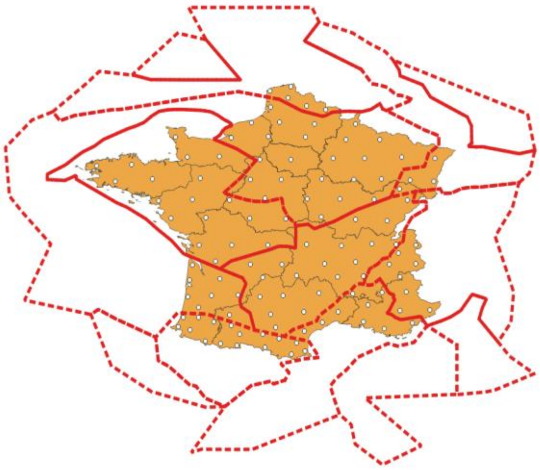

Figure 10: Grid of points selected for risk calculation within each domain

A median value was then calculated for each domain. These results are presented in the next section. For every of the 6 combinations of hazard and fragility, the calculated seismic risk exhibits a strong consistency:

- The larger the damage grade, the lower its probability of occurrence,
- The larger the vulnerability class, the lower the expected damage,
- The seismic risk is lower for stables domains (ex. “plateforme stable continentale”, domain No 7) and higher for more active domains (ex. “Alpes and Pyrenes, domains 1 and 8).

3.3 Comparing seismic risk evaluations and discussion

This section presents the comparison of two seismic risk described in the precedents sections: 1) seismic risk derived from historical seismicity and 2) seismic risk derived from seismic hazard maps and fragility curves. Results are summarized in the table 7. They are also presented in the form of graphs. As an example, the figure 9 shows the comparison for the domain 1 (Alps + Base). The graphs of other domains are in Annex 2.

	D2				D3				D4			
	MEED	SHARE	GEOTER	HISTORIQUE	MEED	SHARE	GEOTER	HISTORIQUE	MEED	SHARE	GEOTER	HISTORIQUE
ALPES + BALE	6,10E-02	4,61E-02	2,52E-03	5,26E-04	1,34E-02	8,04E-03	1,13E-03	9,22E-05	3,23E-03	1,59E-03	5,21E-04	1,52E-05
BLOC ARMORICAIN	1,51E-02	1,63E-03	6,10E-04	3,16E-05	3,33E-03	3,80E-04	3,40E-04	3,96E-06	8,03E-04	9,62E-05	1,99E-04	4,58E-07
GRABEN DU RHIN	3,51E-02	3,03E-02	1,11E-03	6,90E-05	7,71E-03	4,44E-03	4,58E-04	4,06E-07	1,86E-03	7,58E-04	1,95E-04	2,39E-09
MANCHE / MER DU NORD	1,26E-02	1,95E-03	2,80E-04	4,20E-05	2,76E-03	4,55E-04	1,57E-04	9,65E-07	6,65E-04	1,15E-04	8,86E-05	2,21E-08
MASSIF CENTRAL / BRESSE / JURA	1,42E-02	3,44E-03	3,72E-04	5,73E-06	3,13E-03	5,66E-04	1,90E-04	1,15E-07	7,54E-04	1,33E-04	8,76E-05	2,31E-09
MEDITERRANEE	1,39E-02	4,19E-03	4,86E-04	1,38E-04	3,06E-03	9,76E-04	2,31E-04	3,95E-05	7,38E-04	2,47E-04	1,12E-04	9,99E-06
PLATEFORME STABLE OCCIDENTALE	2,70E-03	3,65E-04	2,81E-04	3,88E-07	5,95E-04	1,42E-04	1,67E-04	7,81E-09	1,43E-04	5,70E-05	9,93E-05	1,56E-10
PYRENEES	3,08E-02	1,00E-02	1,73E-03	5,21E-04	6,78E-03	2,08E-03	6,46E-04	3,94E-05	1,63E-03	4,78E-04	2,50E-04	7,16E-07
FRANCE CONTINENTALE	1,47E-02	5,43E-03	6,16E-04	7,92E-05	3,23E-03	1,01E-03	3,03E-04	1,12E-05	7,79E-04	2,23E-04	1,54E-04	1,75E-06

a. Murphy & O'Brien 1977 – Vulnerability class B

	D2				D3				D4			
	MEED	SHARE	GTR	HISTORIQUE	MEED	SHARE	GTR	HISTORIQUE	MEED	SHARE	GTR	HISTORIQUE
ALPES + BALE	2,61E-02	1,66E-02	1,72E-03	5,26E-04	6,70E-03	3,47E-03	8,34E-04	9,22E-05	1,94E-03	8,49E-04	4,23E-04	1,52E-05
BLOC ARMORICAIN	6,49E-03	7,28E-04	4,59E-04	3,16E-05	1,66E-03	1,96E-04	2,80E-04	3,96E-06	4,83E-04	5,95E-05	1,68E-04	4,58E-07
Graben du Rhin	1,50E-02	9,47E-03	7,21E-04	6,90E-05	3,85E-03	1,71E-03	3,23E-04	4,06E-07	1,12E-03	3,68E-04	1,53E-04	2,39E-09
MANCHE / MER DU NORD	5,38E-03	8,72E-04	2,16E-04	4,20E-05	1,38E-03	2,35E-04	1,27E-04	9,65E-07	4,00E-04	7,12E-05	7,72E-05	2,21E-08
MASSIF CENTRAL / BRESSE / JURA	6,09E-03	8,72E-04	2,75E-04	5,73E-06	1,56E-03	2,35E-04	1,42E-04	1,15E-07	4,53E-04	7,12E-05	7,06E-05	2,31E-09
MEDITERRANEE	5,96E-03	1,87E-03	3,43E-04	1,38E-04	1,53E-03	5,05E-04	1,75E-04	3,95E-05	4,44E-04	1,53E-04	9,28E-05	9,99E-06
PLATEFORME STABLE OCCIDENTALE	1,16E-03	2,29E-04	2,23E-04	3,88E-07	2,97E-04	9,73E-05	1,38E-04	7,81E-09	8,62E-05	4,39E-05	8,80E-05	1,56E-10
PYRENEES	1,32E-02	4,12E-03	1,06E-03	5,21E-04	3,39E-03	1,00E-03	4,34E-04	3,94E-05	9,82E-04	2,79E-04	1,90E-04	7,16E-07
FRANCE CONTINENTALE	6,29E-03	1,96E-03	4,39E-04	7,92E-05	1,61E-03	4,59E-04	2,33E-04	1,12E-05	4,68E-04	1,27E-04	1,28E-04	1,75E-06

b. Faccioli & Cauzzi 2006 – Vulnerability class B

	D2				D3				D4			
	MEED	SHARE	GEOTER	HISTORIQUE	MEED	SHARE	GEOTER	HISTORIQUE	MEED	SHARE	GEOTER	HISTORIQUE
ALPES + BALE	1,32E-02	7,95E-03	1,11E-03	9,22E-05	2,85E-03	1,36E-03	4,96E-04	1,52E-05	6,84E-04	2,67E-04	2,28E-04	1,60E-06
BLOC ARMORICAIN	3,28E-03	3,74E-04	3,35E-04	3,96E-06	7,07E-04	8,54E-05	1,93E-04	4,58E-07	1,70E-04	2,16E-05	9,68E-05	3,72E-08
GRABEN DU RHIN	7,60E-03	4,41E-03	4,50E-04	4,06E-07	1,64E-03	6,31E-04	1,84E-04	2,39E-09	3,93E-04	1,07E-04	7,79E-05	1,37E-11
MANCHE / MER DU NORD	2,72E-03	4,48E-04	1,54E-04	9,65E-07	5,86E-04	1,02E-04	8,58E-05	2,21E-08	1,41E-04	2,58E-05	4,84E-05	4,61E-10
MASSIF CENTRAL / BRESSE / JURA	3,08E-03	5,61E-04	1,87E-04	1,15E-07	6,64E-04	1,17E-04	8,33E-05	2,31E-09	1,60E-04	2,82E-05	3,74E-05	4,27E-11
MEDITERRANEE	3,02E-03	9,61E-04	2,27E-04	3,95E-05	6,50E-04	2,20E-04	1,07E-04	9,99E-06	1,56E-04	5,55E-05	5,19E-05	1,42E-06
PLATEFORME STABLE OCCIDENTALE	5,86E-04	1,39E-04	1,64E-04	7,81E-09	1,26E-04	5,35E-05	9,65E-05	1,56E-10	3,03E-05	2,14E-05	5,75E-05	2,89E-12
PYRENEES	6,67E-03	2,05E-03	6,35E-04	3,94E-05	1,44E-03	4,18E-04	2,34E-04	7,16E-07	3,46E-04	9,46E-05	9,04E-05	1,21E-08
FRANCE CONTINENTALE	3,18E-03	9,94E-04	2,99E-04	1,12E-05	6,86E-04	1,94E-04	1,48E-04	1,75E-06	1,65E-04	4,53E-05	7,32E-05	2,05E-07

c. Murphy & O'Brien 1977 – Vulnerability class C

	D2				D3				D4			
	MEED	SHARE	GEOTER	HISTORIQUE	MEED	SHARE	GEOTER	HISTORIQUE	MEED	SHARE	GEOTER	HISTORIQUE
ALPES + BALE	6,51E-03	3,36E-03	8,21E-04	9,22E-05	1,72E-03	7,29E-04	4,04E-04	1,52E-05	4,89E-04	1,74E-04	2,03E-04	1,60E-06
BLOC ARMORICAIN	1,62E-03	1,91E-04	2,77E-04	3,96E-06	4,27E-04	5,31E-05	1,61E-04	4,58E-07	1,21E-04	1,58E-05	9,09E-05	3,72E-08
Graben du Rhin	3,74E-03	1,64E-03	3,18E-04	4,06E-07	9,89E-04	3,08E-04	1,45E-04	2,39E-09	2,81E-04	6,47E-05	6,80E-05	1,37E-11
MANCHE / MER DU NORD	1,34E-03	2,29E-04	1,26E-04	9,65E-07	3,54E-04	6,35E-05	7,49E-05	2,21E-08	1,01E-04	1,89E-05	4,52E-05	4,61E-10
MASSIF CENTRAL / BRESSE / JURA	1,52E-03	2,29E-04	1,40E-04	1,15E-07	4,01E-04	6,35E-05	6,73E-05	2,31E-09	1,14E-04	1,89E-05	3,32E-05	4,27E-11
MEDITERRANEE	1,49E-03	4,91E-04	1,72E-04	3,95E-05	3,93E-04	1,36E-04	8,90E-05	9,99E-06	1,12E-04	4,05E-05	4,68E-05	1,42E-06
PLATEFORME STABLE OCCIDENTALE	2,89E-04	9,56E-05	1,37E-04	7,81E-09	7,63E-05	4,14E-05	8,57E-05	1,56E-10	2,17E-05	1,84E-05	5,41E-05	2,89E-12
PYRENEES	3,29E-03	9,74E-04	4,26E-04	3,94E-05	8,70E-04	2,45E-04	1,78E-04	7,16E-07	2,47E-04	6,36E-05	7,68E-05	1,21E-08
FRANCE CONTINENTALE	1,57E-03	4,45E-04	2,30E-04	1,12E-05	4,15E-04	1,12E-04	1,23E-04	1,75E-06	1,18E-04	3,18E-05	6,70E-05	2,05E-07

d. Faccioli & Cauzzi 2006 – Vulnerability class C

Table 7: Annual probabilities of having a damage greater or equal to degrees D2, D3 and D4 using: a) Murphy & O'Brien 1977 and vulnerability class B; b) Faccioli & Cauzzi 2006 and vulnerability class B; c) Murphy & O'Brien 1977 and vulnerability class C; d) Faccioli & Cauzzi 2006 and vulnerability class C. Results from each seismic hazard map is indicated in the table by MEED, SHARE, GEOTER. The seismic risk based on historical seismicity is indicated in the colomn HISTORIQUE.

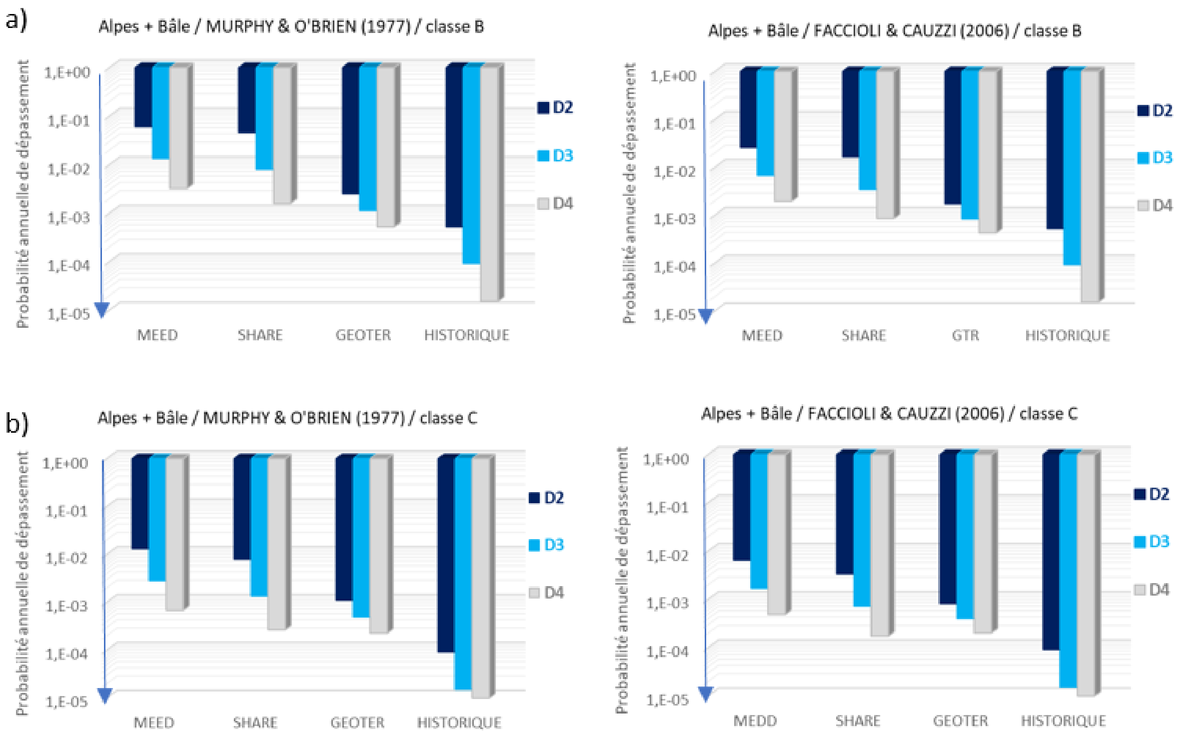

Figure 11: Comparison of the seismic risk derived from seismic hazard maps (MEED, SHARE, GEOTER) and seismic risk based on historical seismicity, horizontal scale. a) Seismic risk for vulnerability class B and b) Seismic risk for vulnerability class C using Murphy & O'Brien (1997) in the left and Faccioli & Cauzzi (2006) in the right side. The dark blue, light blue and the grey colours represent respectively the degrees of damages D2, D3 and D4.

The most remarkable output of this research is that the seismic risk derived from convolution of seismic hazard maps and fragility curves is systematically and significantly larger, by one or two orders of magnitude, than the seismic risk derived from historical seismicity. This tendency is obtained for all type of hazard models, hypothesis, vulnerability and degree of damage tested.

Regarding the three considered hazard maps, the seismic risk derived from the MEDD map is the highest in the vast majority of case, followed by the SHARE map, and finally the seismic risk of GEOTER map remains the lowest. Therefore, the GEOTER map is the most consistent with the historical seismic risk and the MEDD map is the less consistent.

Regarding activity domains, it is interesting to note that the gap between the two risk approaches is much smaller in the most active domain (Pyrénées) than in the less active one (Plateforme stable).

Regarding the two considered conversions formulas, the one by Faccioli and Cauzzi leads to risk estimates that are systematically more consistent with the historical risk than the one by Murphy and O'Brien.

Regarding vulnerability classes and damage grades, it is observed that selecting class B and damage D2 trends to minimize the gap between the two seismic risk approaches.

A satisfactory consistency between the two approaches is obtained in the following case:

- Pyrénées Domain,
- GEOTER map,
- Vulnerability B,
- Damage D2,
- Conversion formula by Faccioli and Cauzzi,

which leads to:

- Risk estimate 1 (historical seismicity): 5.21 10^{-4},
- Risk estimate 2 (convolution hazard-fragility): 10.6 10^{-4}.

4 Conclusions and perspectives

This research applied a methodology based on macroseismic data to check the consistency of three hazard maps of the French metropolitan territory (MEED, SHARE, GEOTER). The methodology consists in calculating the seismic risk using two different approaches: 1) seismic risk derived from historical seismicity and 2) seismic risk calculated by convolution of hazard maps and fragility curves.

The main output of this research is that the seismic risk derived from convolution of seismic hazard maps and fragility curves is systematically and significantly larger, by one or two orders of magnitude, than the seismic risk derived from historical seismicity. This tendency is obtained for all type of hazard models, hypothesis, vulnerability and degree of damage tested.

The seismic risk calculated with the GEOTER map is the less inconsistent with the seismic risk derived from historical seismicity, the MEDD map is the most inconsistent. These results highlight that, among the three models tested in the present study, GEOTER model is the one that should relatively be regarded as the most coherent with observations of historical seismicity.

Although some developments of the presented analyses are still possible, it is not expected that the gap between the two approaches could be bridged at the current state of practice. Main tracks of development are as follows:

- Fragility curves

At the moment when this study was conducted, fragility curves directly established in PGA for well characterized EMS-98 vulnerability classes are not available. Available curves explicitly associated to vulnerability classes were obtained through intensity-PGA conversion formula, while curves directly established in PGA were not associated to a vulnerability class. For the beauty of the analysis, it would be preferable that fragility curves directly established in PGA (without conversion formula) be available for EMS-98 vulnerability classes. However, the sensitivity study conducted in this study gives evidence that, in practice, only a small part of the gap between approaches could be bridged through a new fragility curve.

- Site amplification factors

Hazard data used in this study are those corresponding to rock sites. Of course, it is not possible to assume that the entire France is made of rocky sites. In practice it would be necessary that the building stock distribution in sites categories (e.g. Eurocode 8 categories) be accounted for through a site amplification factor. This necessary development can only lead to enlarging the gap between approaches.

- Expected maximum intensities

As indicated above, although there was no observation of intensity 9 in the French continental territory during the considered period of time, it is not possible to derive that the probability of such an event is zero. To cope with this issue, an inclusive extrapolation has been implemented, based on expert judgment. In the future it is expected that, the extreme value theory will be used to derive an extreme intensity frequency, in a manner similar to the one used by Dutfoy (2019) for extreme magnitudes.

- Uncertainties

In this study uncertainties on the distribution of seismic event on a century, as well as uncertainties on isoseismal have not been evaluated or processed. They could be both addressed in further developments. Another option to handle uncertainties would be that fractiles of hazard maps are examined in addition to the median map. Such an analysis could for instance lead to the conclusion that the fractile 20% or 30% of a given map is consistent with historical seismicity.

5 References

Albarello D. and V., D'Amico (2008): Testing probabilistic seismic hazard estimates by comparison with observations; an example in Italy. Geophysical Journal International, Vol. 175, No. 3, pp. 1088-1094.

Brune J.N.(2002): Precarious-rock constraints on ground motion from historic and recent earthquakes in Southern California, Bulletin of the Seismological Society of America, Vol. 92, No. 7, pp. 2602-2611.

Drouet S., Le Dortz K., Secanell R., Ameri G. (2017): Probabilistic seismic maps for the French metropolitan territorry. Ref: GTR/EDF/0517-1603. Publication in progress.

Dutfoy A. (2019): Estimation of Tail Distribution of the Annual Maximum Earthquake Magnitude using Extreme Value Theory. PAAG, Volume 176, Issue 2, pp 527–540.

Faccioli & Cauzzi (2006): Macroseismic intensities for seismic scenarios, estimated from instrumentally based correlations. First European Conference on Earthquake Engineering and Seismology, Geneva.

Fujiwara H., Morikawa N., Y., Ishikawa, T., Okumura, J., Miyakoshi, N., Nojima, and Y., Fukushima, (2019): Statistical comparison of National Probabilistic Seismic Hazard Maps and frequency of recorded JMA seismic intensities from the K-NET strong-motion observation network in Japan during 1997-2006, Seismological Research Letters, Vol. 80, No. 3 (2009).

Grünthal G (1998): European Macroseismic Scale 1998 (EM98). Edition A. LEVRET

J. Lambert, A. Levret (1996): Mille ans de séismes en France, Ouest-Editions.

Kennedy R. (1999). Overview of methods for seismic PRA and margin analysis, including recent innovations. OECD-NEA workshop on seismic risk, Tokyo.

Labbé P. (2018): Statistical treatment of a comprehensive set of isoseismals observed in France during one century. 16th European conference on Earthquake engineering, Thessaloniki.

Labbé P.(2008): Comparison of two methods of seismic assessment in France, 14th World Conference on Earthquake Engineering, Beijing, China (2008).

Labbé P.(2010): PSHA outputs versus historical seismicity, example of France, 14th European Conference of Earthquake Engineering, Ohrid, FYROM (2010).

Labbé P.(2017): PSHA testing against historical seismicity Example of France. 16th World Conference on Earthquake, Santiago Chile.

Lagomarsino S. & Cattari S. (2014): Fragility Functions of Masonry Buildings. SYNER-G: Typology Definition and Fragility Functions for Physical Elements at Seismic Risk, Vol 27.

Lambert J., Monfort D., Bouc O. (2015): Catalogue of isoseismal areas for xxth century French historical earthquakes (Io > VI). SIGMA report – Ref SIGMA-D1-148.

Levret A., Backe C., Cushing M. (1994): Atlas of Macroseismic Maps for French Earthquakes with Their Principal Characteristics. *Natural Hazards* **10:** 19-46, 1994

Martin Ch., Ameri G., Baumont D., Carbon D., Senfaute G., Thiry J.M., E. Faccioli, J. Savy (2017): Probabilistic seismic hazard assessment for South-Eastern France. Bull Earthquake Eng. DOI 10.1007/s10518-017-0249-9

Milutinovic Z. V. & Trendafiloski G. S. (2003): An advanced approach to earthquake risk scenarios with applications to different European towns. RISK-UE WP4 Handbook: Vulnerability of current buildings.

Murphy J.R. & O'Brien L.J. (1977): The correlation of peak ground acceleration amplitudes with seismic intensity and other physical parameters. BSSA 67(3).

OECD/NEA (2015): Workshop on Testing Probabilistic Seismic Hazard Analysis Results and the Benefits of Bayesian Techniques. Pavia February 2015, Nuclear Safety NEA/CSNI/R (2015).

Pecker A., E. Faccioli, A. Gurpinar, Ch. Martin, Ph. Renault, (2017): An overview of the SIGMA research project, Springer.

Rey J., Beauval C. & Douglas J. (2018): Do French macroseismic intensity observations agree with expectations from the European Seismic Hazard Model 2013? J. Seismol. https://doi.org/10.1007/s10950-017-9724-7

Rota M., Penna A. & Magenes G. (2008): A Procedure for Deriving Analytical Fragility Curves for Masonry Buildings. The 14th World Conference on Earthquake Engineering, Beijing.

Senfaute G, Pecker A., Labbé P., JF Sidaner, c. Berge-THierry, JP Rzepka, P. Contri (2015): Contribution of the SIGMA research programme to analyses of uncertainties in seismic hazard assessment, 9e Colloque National, AFPS, France, 2015

Stein, S., Opinion: Bad Assumptions or Bad Luck: Why earthquake hazard maps need objective testing, Seismological Research Letters, Vol. 82, No. 5 (2011)

Stirling, M.W. and M.C. (2010): Gerstenberger, Ground motion-based testing of seismic hazard models in New Zealand, Bulletin of the Seismological Society of America, Vol. 100, No. 4, pp. 1407-1414 (2010).

Stirling M.W. and Petersen M.D (2006): Comparison of the historical record of earthquake hazard with seismic hazard models for New Zealand and the continental United States, Bulletin of the Seismological Society of America, Vol. 96, pp. 1978-1994.

Stirling M.W. (2012): Opinion: Earthquake hazard maps and objective testing: The hazard mapper's point of view, Seismological Research Letters, Vol. 83, No. 2.

TecDoc IAEA (International Atomic Energy Agency) - Evaluating probabilistic seismic hazard analysis based on observations. TecDoc IAEA in progress.

Viallet E., Humbert N., Martin C., and Secanell R. (2008): On the use of a Bayesian updating technique to get probabilistic seismic hazard assessment more rugged, 14th World Conference on Earthquake Engineering, Beijing, China (2008).

ANNEX 1 - Description of fragility curves parameters

To obtain the parameters a_D and β_D, the approach of LAGOMARSINO & GIOVINAZZI (2006), taken up by LAGOMARSINO & CATTARI (2014) is used.

This approach consists in translating the EMS-98 scale based on macroseismic intensities from the fuzzy sets theory. A mean damage function in intensities is obtained. Then a fragility curve using a binomial distribution is obtained in intensities. After converting the curves from intensities to PGA, a calibration of these curves on a log-normal distribution is performed to obtain the parameters a_D and β_D,

The mean damage functions are given by the following formula:

$$\mu_{\mathcal{C}}(I) = \begin{cases} 2.5 + 3\,tanh\left(\dfrac{I + 6.25V_{\mathcal{C}} - 12.7}{Q}\right) & I > 7 \qquad (A1.1) \\ \left[2.5 + 3\,tanh\left(\dfrac{I + 6.25V_{\mathcal{C}} - 12.7}{Q}\right)\right] e^{\frac{V_{\mathcal{C}}(I-7)}{2}} & I \leq 7 \qquad (A1.2) \end{cases}$$

Where :

$V_{\mathcal{C}}$: vulnerability index for vulnerability class $\mathcal{C}$,

Q : ductility index.

These two parameters characterize the seismic behavior of a homogeneous set of buildings.

Table A1.1 presents the ranges of possible values of this index for the vulnerability classes A to D (representative of the masonry) obtained from the theory of the fuzzy sets:

$\boldsymbol{\mathcal{C}}$	A	B	C	D
$\boldsymbol{V_{\mathcal{C}}}$	$[0.84 - 0.92]$	$[0.68 - 0.76]$	$[0.52 - 0.60]$	$[0.36 - 0.44]$

Table A1.1: Vulnerability index values proposed by LAGOMARSINO & CATTARI (2014)

Following values were selected for calculations: $V_A = 0.88$; $V_B = 0.72$; $V_C = 0.56$; $V_D = 0.40$; and the ductility index, was calibrated to 3. Figure A1.1 shows the corresponding pseudo-fragility curves for the A to D classes.

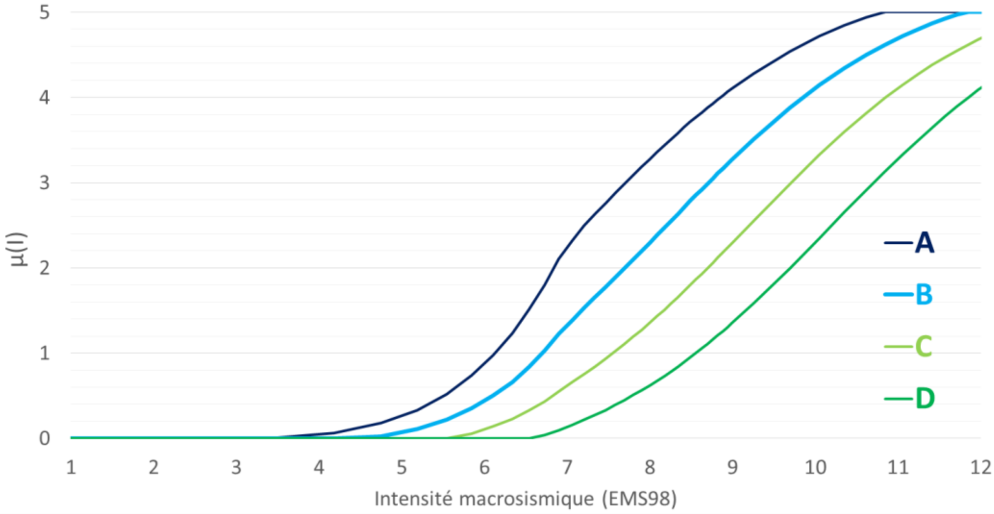

Figure A1.1: Mean damage curves for the vulnerability classes A to D

From these mean damage functions, one can have the probability $f_D^{\mathcal{C}}(I)$ of having a damage of degree D on a building of vulnerability class $\mathcal{C}$ caused by a felt intensity I. This probability is assumed to be binomially distributed $\mathcal{B}\left(5.\frac{\mu_D(I)}{5}\right)$.

$$f_D^{\mathcal{C}}(I) = \frac{5!}{D!\,(5-D)!}\left(\frac{\mu_{\mathcal{C}}(I)}{5}\right)^D\left(1-\frac{\mu_{\mathcal{C}}(I)}{5}\right)^{5-D} \qquad \text{(A1.3)}$$

Thus, the probability$F_D^{\mathcal{C}}(I)$ to have a damage greater than or equal to D on a building of vulnerability class $\mathcal{C}$ caused by a felt intensity I is given by the formula (A1.4):

$$F_D^{\mathcal{C}}(I) = \sum_{k=D}^{5} f_k^{\mathcal{C}}(I) \qquad \text{(A1.4)}$$

However, these fragility curves are functions of the macroseismic intensity whereas we need curves in accelerations (PGA).

To do this, two PGA-macroseismic intensity conversion formulas were used namely those of MURPHY & O'BRIEN (1977) and FACCIOLI & CAUZZI (2006). The equation (A1.5) gives the standard form of these formulas:

$$I = a + b\,log(PGA) \qquad \text{(A1.5)}$$

Table A1.2 presents the values of a and b proposed by MURPHY & O'BRIEN (1977) and FACCIOLI & CAUZZI (2006) and the corresponding formulas are plotted in Figure A1.2

	a	b
MURPHY & O'BRIEN (1977)	7	4
FACCIOLI & CAUZZI (2006)	6.54	4.51

Table A1.2: Parameter values of the intensity – PGA conversions formulas

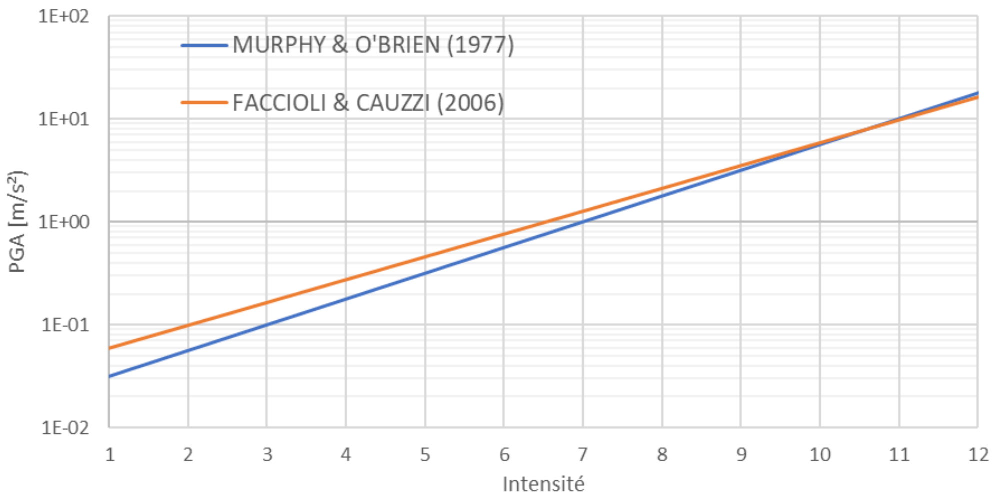

Figure A1.2: Representation of the conversion formulas

It only remains to convert the intensities in PGA to get the fragility curves in PGA. For the rest, only the degrees of damage 2, 3 and 4 were selected for this study. In addition, only vulnerability classes B and C of the EMS-98 scale were analyzed. Figures A1.3 and A1.4 present the fragility curves derived from both considered conversion formulas.

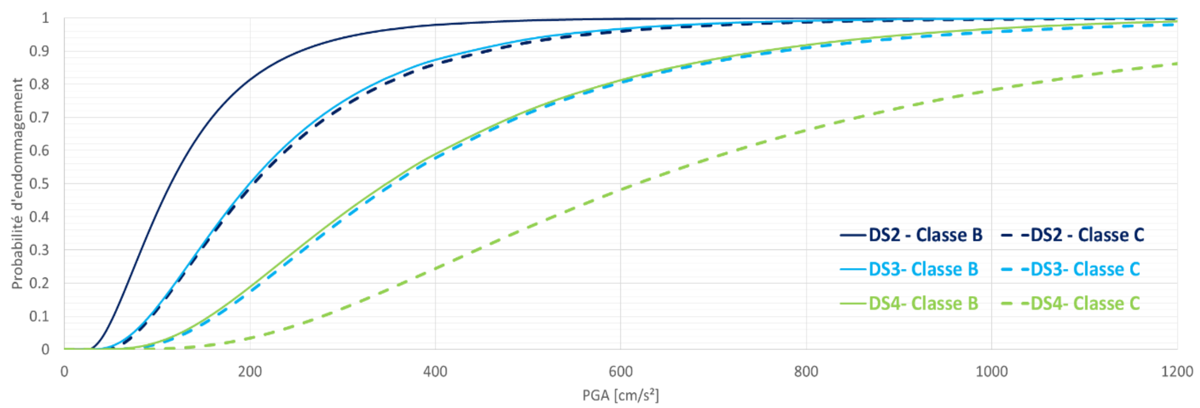

Figure A1.3: Fragility curves for vulnerability classes B and C based on MURPHY & O'BRIEN (1977)

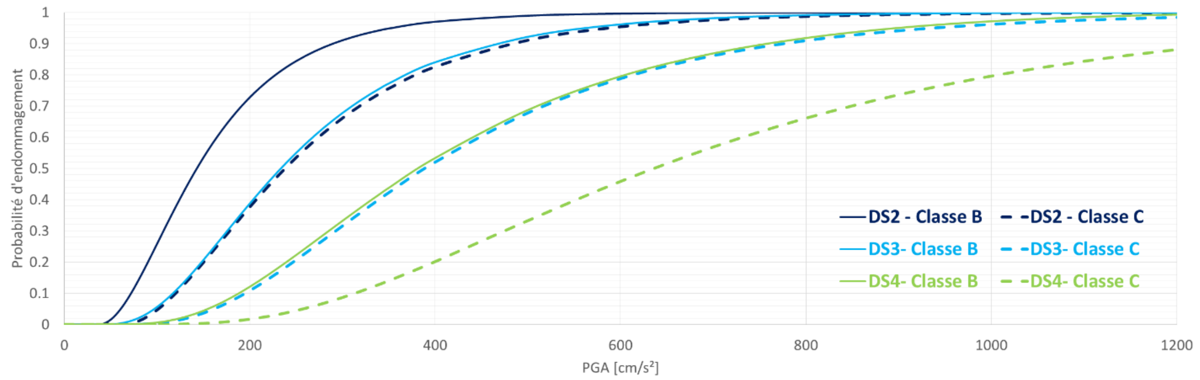

Figure A1.4: Fragility curves for vulnerability classes B and C
based on FACCIOLI & CAUZZI (2006),

Values of a_D were obtained as the median of each series. Values of β_D they were obtained by calibration so that the curves of figures A1.3 and A1.4 are as close as possible to a log-normal curve.

ANNEX 2 - Seismic risk comparison

Comparison of the seismic risk derived from seismic hazard maps (MEED, SHARE, GEOTER) and seismic risk based on historical seismicity, horizontal scale. a) Seismic risk for vulnerability class B and b) Seismic risk for vulnerability class C using Murphy & O'Brien (1997) in the left and Faccioli & Cauzzi (2006) in the right side. The blue colours and the grey colour represent respectively the degrees of damages D2, D3 and D4

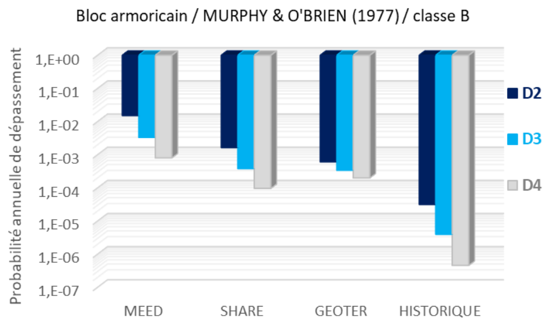

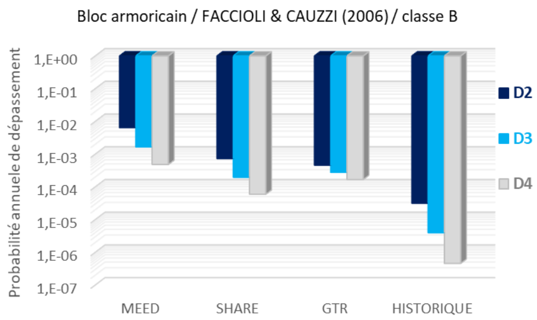

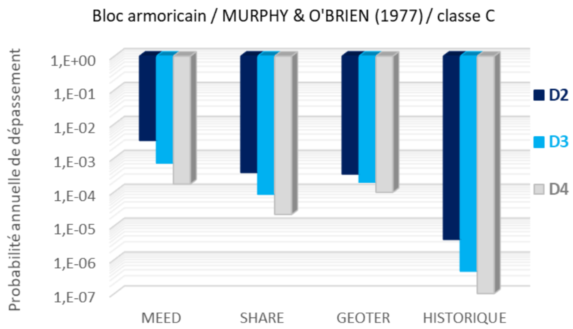

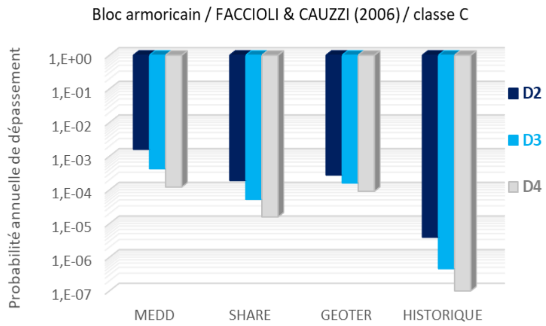

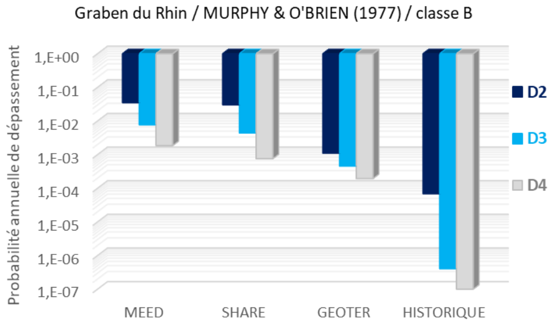

Graben du Rhin / MURPHY & O'BRIEN (1977) / classe B
Probabilité annuelle de dépassement
1,E+00
1,E-01
1,E-02
1,E-03
1,E-04
1,E-05
1,E-06
1,E-07
MEED
SHARE
GEOTER
HISTORIQUE
D2
D3
D4

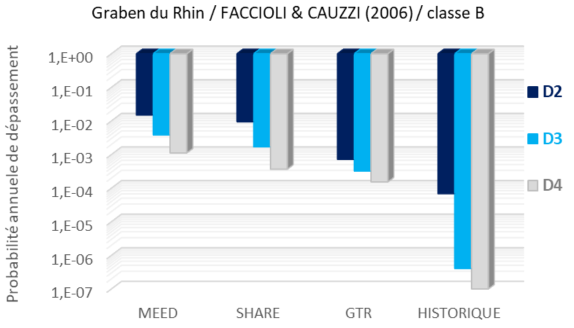

Graben du Rhin / FACCIOLI & CAUZZI (2006) / classe B
Probabilité annuelle de dépassement
1,E+00
1,E-01
1,E-02
1,E-03
1,E-04
1,E-05
1,E-06
1,E-07
MEED
SHARE
GTR
HISTORIQUE
D2
D3
D4

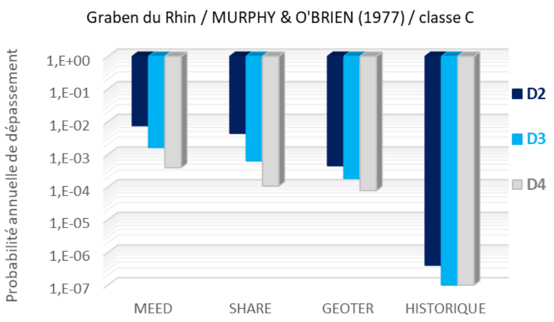

Graben du Rhin / MURPHY & O'BRIEN (1977) / classe C
Probabilité annuelle de dépassement
1,E+00
1,E-01
1,E-02
1,E-03
1,E-04
1,E-05
1,E-06
1,E-07
MEED
SHARE
GEOTER
HISTORIQUE
D2
D3
D4

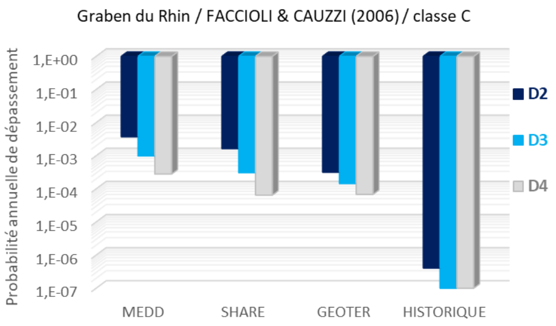

Graben du Rhin / FACCIOLI & CAUZZI (2006) / classe C
Probabilité annuelle de dépassement
1,E+00
1,E-01
1,E-02
1,E-03
1,E-04
1,E-05
1,E-06
1,E-07
MEDD
SHARE
GEOTER
HISTORIQUE
D2
D3
D4

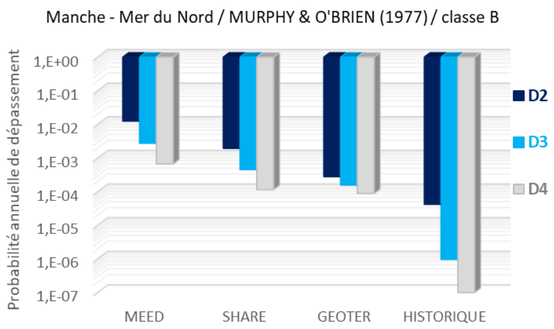

Manche - Mer du Nord / MURPHY & O'BRIEN (1977) / classe B
Probabilité annuelle de dépassement
1,E+00
1,E-01
1,E-02
1,E-03
1,E-04
1,E-05
1,E-06
1,E-07
MEED
SHARE
GEOTER
HISTORIQUE
D2
D3
D4

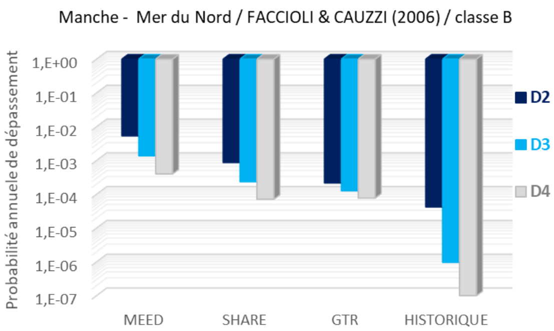

Manche - Mer du Nord / FACCIOLI & CAUZZI (2006) / classe B
Probabilité annuelle de dépassement
1,E+00
1,E-01
1,E-02
1,E-03
1,E-04
1,E-05
1,E-06
1,E-07
MEED
SHARE
GTR
HISTORIQUE
D2
D3
D4

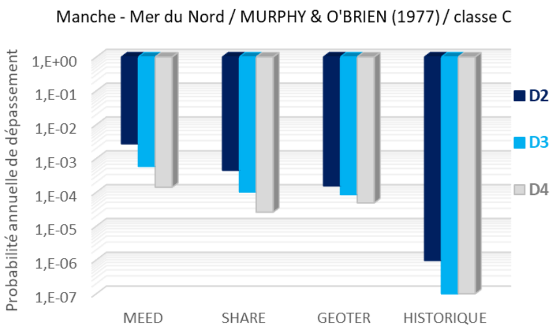

Manche - Mer du Nord / MURPHY & O'BRIEN (1977) / classe C
Probabilité annuelle de dépassement
1,E+00
1,E-01
1,E-02
1,E-03
1,E-04
1,E-05
1,E-06
1,E-07
MEED
SHARE
GEOTER
HISTORIQUE
D2
D3
D4

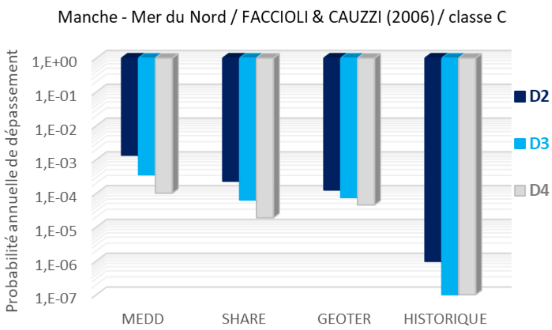

Manche - Mer du Nord / FACCIOLI & CAUZZI (2006) / classe C
Probabilité annuelle de dépassement
1,E+00
1,E-01
1,E-02
1,E-03
1,E-04
1,E-05
1,E-06
1,E-07
MEDD
SHARE
GEOTER
HISTORIQUE
D2
D3
D4

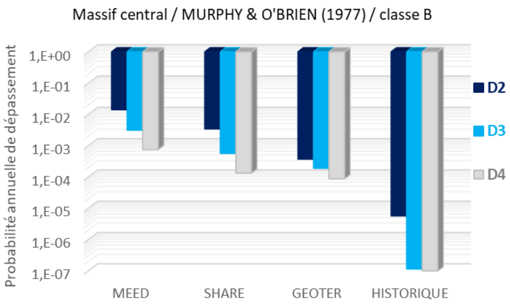
Massif central / MURPHY & O'BRIEN (1977) / classe B
Probabilité annuelle de dépassement
1,E+00
1,E-01
1,E-02
1,E-03
1,E-04
1,E-05
1,E-06
1,E-07
MEED
SHARE
GEOTER
HISTORIQUE
D2
D3
D4

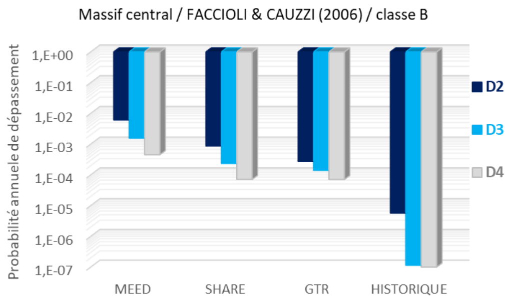
Massif central / FACCIOLI & CAUZZI (2006) / classe B
Probabilité annuelle de dépassement
1,E+00
1,E-01
1,E-02
1,E-03
1,E-04
1,E-05
1,E-06
1,E-07
MEED
SHARE
GTR
HISTORIQUE
D2
D3
D4

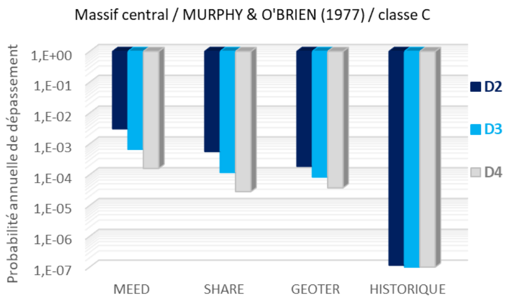
Massif central / MURPHY & O'BRIEN (1977) / classe C
Probabilité annuelle de dépassement
1,E+00
1,E-01
1,E-02
1,E-03
1,E-04
1,E-05
1,E-06
1,E-07
MEED
SHARE
GEOTER
HISTORIQUE
D2
D3
D4

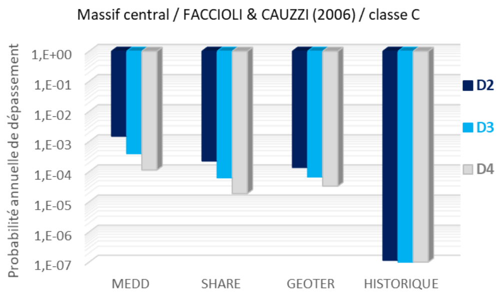
Massif central / FACCIOLI & CAUZZI (2006) / classe C
Probabilité annuelle de dépassement
1,E+00
1,E-01
1,E-02
1,E-03
1,E-04
1,E-05
1,E-06
1,E-07
MEDD
SHARE
GEOTER
HISTORIQUE
D2
D3
D4

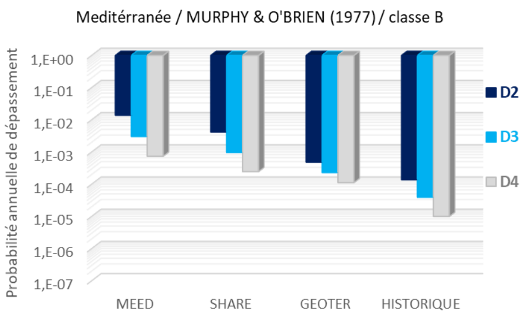
Meditérranée / MURPHY & O'BRIEN (1977) / classe B
Probabilité annuelle de dépassement
1,E+00
1,E-01
1,E-02
1,E-03
1,E-04
1,E-05
1,E-06
1,E-07
MEED
SHARE
GEOTER
HISTORIQUE
D2
D3
D4

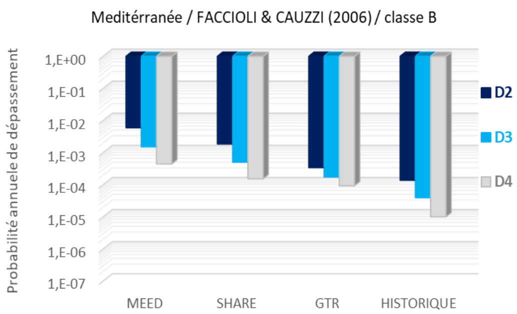
Meditérranée / FACCIOLI & CAUZZI (2006) / classe B
Probabilité annuele de dépassement
1,E+00
1,E-01
1,E-02
1,E-03
1,E-04
1,E-05
1,E-06
1,E-07
MEED
SHARE
GTR
HISTORIQUE
D2
D3
D4

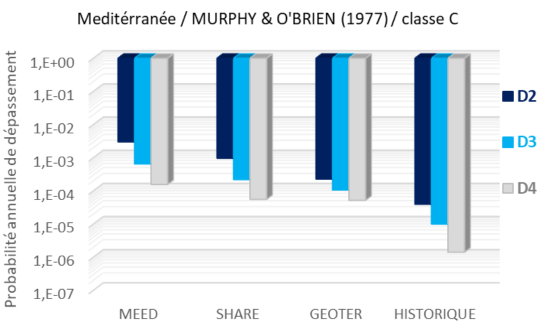
Meditérranée / MURPHY & O'BRIEN (1977) / classe C
Probabilité annuelle de dépassement
1,E+00
1,E-01
1,E-02
1,E-03
1,E-04
1,E-05
1,E-06
1,E-07
MEED
SHARE
GEOTER
HISTORIQUE
D2
D3
D4

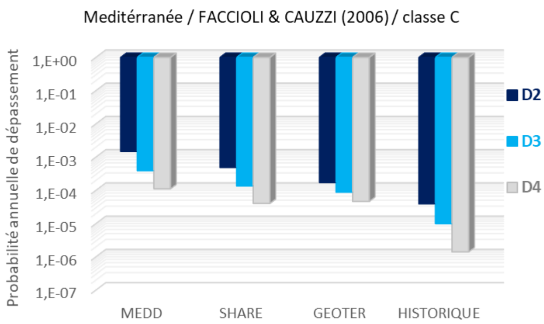
Meditérranée / FACCIOLI & CAUZZI (2006) / classe C
Probabilité annuelle de dépassement
1,E+00
1,E-01
1,E-02
1,E-03
1,E-04
1,E-05
1,E-06
1,E-07
MEDD
SHARE
GEOTER
HISTORIQUE
D2
D3
D4

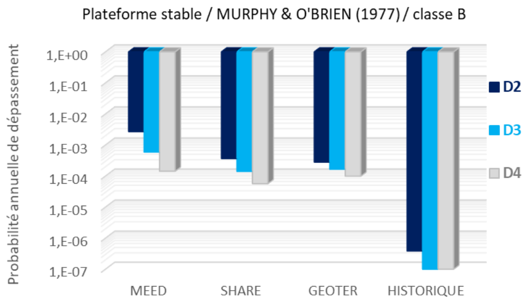
Plateforme stable / MURPHY & O'BRIEN (1977) / classe B
Probabilité annuelle de dépassement
1,E+00
1,E-01
1,E-02
1,E-03
1,E-04
1,E-05
1,E-06
1,E-07
MEED
SHARE
GEOTER
HISTORIQUE
D2
D3
D4

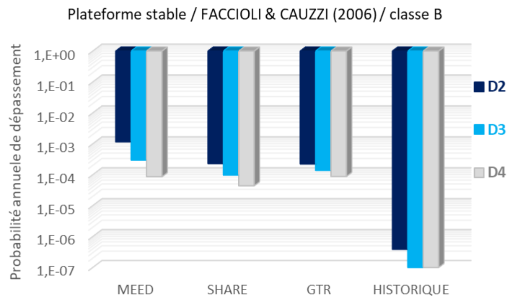
Plateforme stable / FACCIOLI & CAUZZI (2006) / classe B
Probabilité annuele de dépassement
1,E+00
1,E-01
1,E-02
1,E-03
1,E-04
1,E-05
1,E-06
1,E-07
MEED
SHARE
GTR
HISTORIQUE
D2
D3
D4

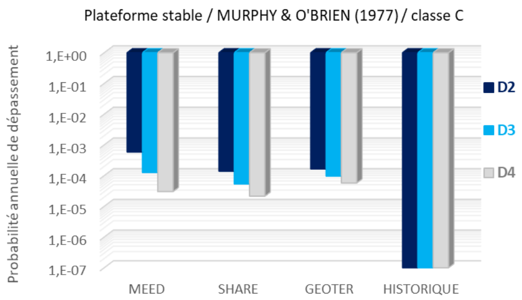
Plateforme stable / MURPHY & O'BRIEN (1977) / classe C
Probabilité annuelle de dépassement
1,E+00
1,E-01
1,E-02
1,E-03
1,E-04
1,E-05
1,E-06
1,E-07
MEED
SHARE
GEOTER
HISTORIQUE
D2
D3
D4

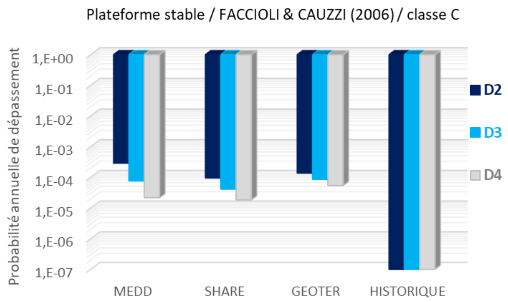
Plateforme stable / FACCIOLI & CAUZZI (2006) / classe C
Probabilité annuelle de dépassement
1,E+00
1,E-01
1,E-02
1,E-03
1,E-04
1,E-05
1,E-06
1,E-07
MEDD
SHARE
GEOTER
HISTORIQUE
D2
D3
D4

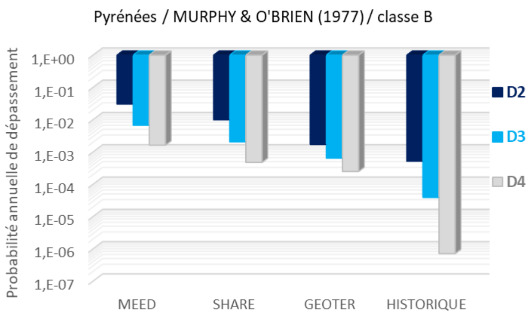
Pyrénées / MURPHY & O'BRIEN (1977) / classe B
Probabilité annuelle de dépassement
1,E+00
1,E-01
1,E-02
1,E-03
1,E-04
1,E-05
1,E-06
1,E-07
MEED
SHARE
GEOTER
HISTORIQUE
D2
D3
D4

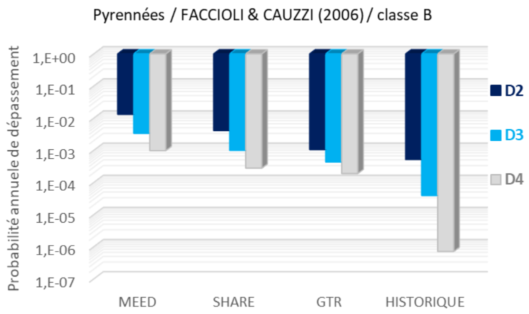
Pyrennées / FACCIOLI & CAUZZI (2006) / classe B
Probabilité annuelle de dépassement
1,E+00
1,E-01
1,E-02
1,E-03
1,E-04
1,E-05
1,E-06
1,E-07
MEED
SHARE
GTR
HISTORIQUE
D2
D3
D4

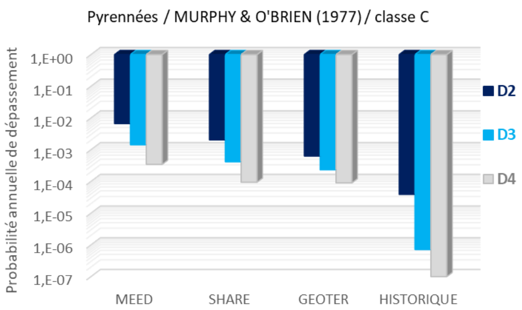
Pyrennées / MURPHY & O'BRIEN (1977) / classe C
Probabilité annuelle de dépassement
1,E+00
1,E-01
1,E-02
1,E-03
1,E-04
1,E-05
1,E-06
1,E-07
MEED
SHARE
GEOTER
HISTORIQUE
D2
D3
D4

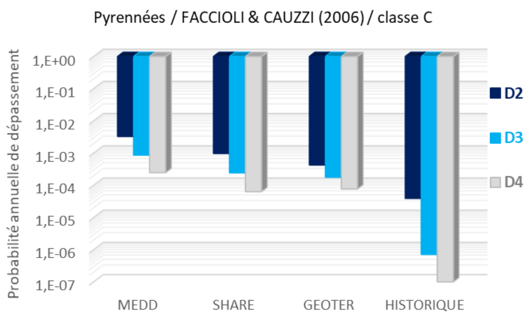
Pyrennées / FACCIOLI & CAUZZI (2006) / classe C
Probabilité annuelle de dépassement
1,E+00
1,E-01
1,E-02
1,E-03
1,E-04
1,E-05
1,E-06
1,E-07
MEDD
SHARE
GEOTER
HISTORIQUE
D2
D3
D4

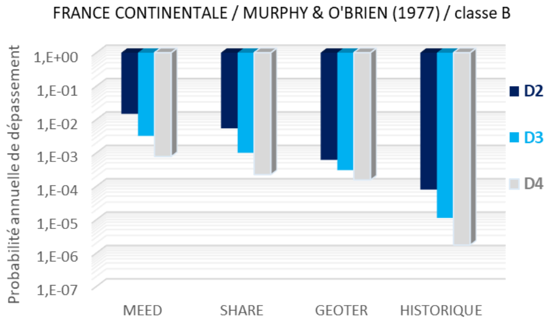
FRANCE CONTINENTALE / MURPHY & O'BRIEN (1977) / classe B
Probabilité annuelle de dépassement
1,E+00
1,E-01
1,E-02
1,E-03
1,E-04
1,E-05
1,E-06
1,E-07
MEED
SHARE
GEOTER
HISTORIQUE
D2
D3
D4

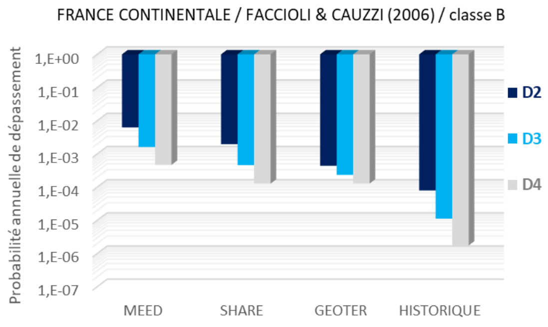
FRANCE CONTINENTALE / FACCIOLI & CAUZZI (2006) / classe B
Probabilité annuelle de dépassement
1,E+00
1,E-01
1,E-02
1,E-03
1,E-04
1,E-05
1,E-06
1,E-07
MEED
SHARE
GEOTER
HISTORIQUE
D2
D3
D4

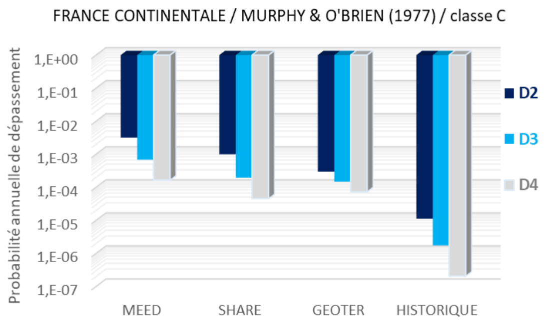
FRANCE CONTINENTALE / MURPHY & O'BRIEN (1977) / classe C
Probabilité annuelle de dépassement
1,E+00
1,E-01
1,E-02
1,E-03
1,E-04
1,E-05
1,E-06
1,E-07
MEED
SHARE
GEOTER
HISTORIQUE
D2
D3
D4

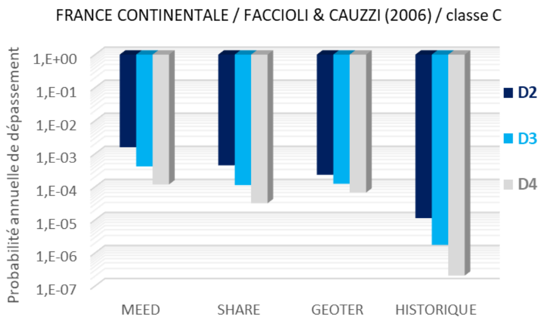
FRANCE CONTINENTALE / FACCIOLI & CAUZZI (2006) / classe C
Probabilité annuelle de dépassement
1,E+00
1,E-01
1,E-02
1,E-03
1,E-04
1,E-05
1,E-06
1,E-07
MEED
SHARE
GEOTER
HISTORIQUE
D2
D3
D4

ANNEX 3 - Grid point coordinates and data for seismic risk calculation

Domain numbering

1	**ALPES + BALE**
2	**BLOC ARMORICAIN / DOMNOMEEN / MANCELLIEN**
3	**GRABEN DU RHIN**
4	**MANCHE / MER DU NORD**
5	**MASSIF CENTRAL / BRESSE / JURA**
6	**MEDITERRANEE**
7	**PLATEFORME STABLE OCCIDENTALE**
8	**PYRENNEES**

Point nb.	Domain number	Long.	Lat.	MEDD a_{ref} cm/s²	MEDD n	SHARE a_{ref} cm/s²	SHARE n	GEOTER a_{ref} cm/s²	GEOTER n
1	1	6.8	46	183.1	2.7	168.9	3.1	120.3	1.44
2	1	5.9	45.3	173.9	2.7	95.8	3.1	77.4	1.44
3	1	6.8	45.4	153.1	2.7	118.6	3.1	94.1	1.44
4	1	6.3	45	154.8	2.7	97.8	3.1	83.0	1.44
5	1	6.5	44.5	185.5	2.7	136.6	3.1	92.5	1.44
6	1	6.3	43.9	164.2	2.7	93.9	3.1	57.1	1.44
7	1	7.3	43.9	177.1	2.7	141.9	3.1	84.8	1.44
8	1	6.2	45.7	174.8	2.7	121.0	3.1	82.1	1.44
9	2	-1.6	49.4	92.6	2.7	44.8	2.6	19.6	0.98
10	2	-1.2	48.8	93.4	2.7	47.5	2.6	23.1	0.98
11	2	-0.1	48.8	85	2.7	41.0	2.6	16.9	1.31
12	2	-4.4	48.5	91.2	2.7	39.6	2.6	24.1	0.98
13	2	-3.2	48.5	93.6	2.7	43.7	2.6	26.2	0.98
14	2	-3.7	48	95.8	2.7	44.8	2.6	31.6	0.98
15	2	-2.4	48.1	94.8	2.7	46.9	2.6	29.1	0.98
16	2	-0.7	48.1	93.7	2.7	46.5	2.6	22.1	1.31
17	2	-2.2	47.4	107.1	2.7	48.7	2.6	35.3	0.98

18	2	-1	47.4	114.1	2.7	48.6	2.6	34.7	0.98
19	2	0.3	47.4	94.7	2.7	42.7	2.6	24.9	1.31
20	2	-1.8	46.8	112.9	2.7	60.3	2.6	36.1	0.98
21	2	-0.6	46.8	116.5	2.7	56.3	2.6	38.5	1.31
22	2	1	46.8	106.6	2.7	47.3	2.6	31.2	1.31
23	2	2.3	46.8	106.3	2.7	48.0	2.6	22.1	1.31
24	2	-0.8	46	116	2.7	56.1	2.6	30.9	0.98
25	2	0.4	46	106.9	2.7	47.6	2.6	29.6	1.31
26	2	1.6	46	104.1	2.7	45.1	2.6	23.3	1.31
27	2	-0.2	45.5	105.3	2.7	44.5	2.6	21.4	1.31
28	3	7.5	48.7	128.9	2.7	90.1	3.4	48.1	1.59
29	3	6.6	48	143.5	2.7	86.5	3.4	46.3	1.59
30	3	7.5	48	150.2	2.7	176.8	3.4	71.3	1.59
31	3	6.3	47.7	140.6	2.7	84.7	3.4	39.6	1.59
32	4	1.7	50.9	95.5	2.7	48.3	2.6	10.8	1.05
33	4	2.4	51	75.1	2.7	73.4	3.1	12.2	1.05
34	4	2.3	50.6	97.1	2.7	46.9	2.5	11.4	1.05
35	4	3	50.4	99.2	2.7	50.2	2.6	16.4	1.05
36	4	3.7	50.3	134.8	2.7	120.5	3.4	29.1	1.05
37	5	6.5	47.4	120.3	2.7	92.2	2.7	52.6	1.2
38	5	4.7	46.8	101.7	2.7	53.5	2.7	19.7	1.2
39	5	5.8	46.7	149.4	2.7	65.0	2.7	50.2	1.2
40	5	3	46	117.7	2.7	94.9	2.7	24.6	1.48
41	5	4.2	46	116.2	2.7	84.1	2.7	18.8	1.2
42	5	5.3	46	124.9	2.7	64.4	2.7	39.6	1.2
43	5	6.1	46	173.9	2.7	128.3	2.7	75.2	1.2
44	5	1	45.4	72.6	2.7	29.2	2.5	16.4	1.48
45	5	2.1	45.4	60.5	2.7	34.0	2.5	15.0	1.48
46	5	3.6	45.4	116.9	2.7	84.3	3.2	18.7	1.2
47	5	4.7	45.4	118.4	2.7	61.4	3.2	28.5	1.2
48	5	1.4	44.9	49.9	2.7	24.2	3.2	12.2	1.48
49	5	2.6	45	87.2	2.7	50.0	3.2	15.6	1.48
50	5	4.1	45	114.2	2.7	73.1	2.7	21.0	1.2
51	5	5	45	155	2.7	94.6	2.7	43.9	1.2
52	5	1.4	44.3	48.7	2.7	25.0	2.5	14.6	1.48
53	5	2.2	44.4	78.4	2.7	35.8	2.5	13.9	1.48
54	5	3.4	44.4	86.1	2.7	45.6	2.7	16.1	1.48

55	5	1.7	43.8	52.3	2.7	30.7	2.5	18.9	1.48
56	5	2.9	43.9	73.6	2.7	35.3	2.7	15.5	1.48
57	5	1.9	43.4	65	2.7	39.8	2.5	25.5	1.48
58	6	4.6	44.4	133.1	2.7	147.4	2.6	31.5	1.34
59	6	5.6	44.5	94	2.7	89.6	2.6	54.5	1.4
60	6	5.2	44.1	130.8	2.7	96.3	2.6	38.5	1.34
61	6	4.1	43.8	93	2.7	37.7	2.6	20.5	1.34
62	6	5	43.5	111.8	2.7	68.8	2.6	25.1	1.34
63	6	2.9	43.2	90.1	2.7	43.7	2.6	25.6	1.34
64	6	5.7	43.3	100.9	2.7	50.3	2.6	24.6	1.4
65	6	6.7	43.5	109.2	2.7	67.4	2.6	37.2	1.44
66	6	3.6	43.5	86.7	2.7	30.9	2.6	18.5	1.34
67	7	1.7	50.3	59	2.7	23.2	1.7	8.0	0.95
68	7	1.1	49.8	49.2	2.7	16.4	1.7	6.9	0.95
69	7	2	49.9	52.8	2.7	19.9	1.7	7.0	0.95
70	7	3.3	49.8	62.3	2.7	30.2	1.7	10.4	0.95
71	7	4.7	49.8	60.4	2.7	33.7	1.7	13.1	0.95
72	7	0.3	49.4	55	2.7	22.1	1.7	11.0	0.95
73	7	1.7	49.4	49	2.7	15.3	1.7	5.8	0.95
74	7	3	49.4	47.2	2.7	18.0	1.7	6.0	0.95
75	7	4.4	49.3	46.9	2.7	19.5	1.7	6.8	0.95
76	7	5.6	49.3	47	2.7	22.2	1.7	10.2	0.95
77	7	1.4	48.7	51.9	2.7	16.5	1.7	6.6	0.95
78	7	2.4	48.7	44.7	2.7	12.6	1.7	4.2	0.95
79	7	3.9	48.7	44.8	2.7	14.0	1.7	4.4	0.95
80	7	5	48.7	46.5	2.7	17.7	1.7	7.1	0.95
81	7	6.3	48.8	56.6	2.7	27.5	1.7	15.1	0.95
82	7	1	48	58.2	2.7	22.4	1.7	10.3	0.95
83	7	2.1	48	48.6	2.7	16.9	1.7	6.5	0.95
84	7	3.5	48.1	47.5	2.7	15.4	1.7	4.7	0.95
85	7	4.7	48	60.3	2.7	26.5	1.7	9.6	0.95
86	7	5.6	48.1	79	2.7	35.3	1.7	16.0	0.95
87	7	1.5	47.4	67.8	2.7	29.3	1.7	14.2	0.95
88	7	3	47.4	69.1	2.7	29.4	1.7	8.0	0.95
89	7	4.2	47.4	62.7	2.7	32.9	1.7	10.4	0.95
90	7	5.4	47.4	82.1	2.7	47.9	1.7	23.9	0.95
91	7	3.5	46.9	67.5	2.7	37.7	1.7	11.2	0.95

92	7	-1.1	44.9	50.5	2.7	20.5	1.7	10.6	0.95
93	7	0	44.9	58.4	2.7	24.4	1.7	12.6	0.95
94	7	-1.2	44.3	50.6	2.7	25.4	1.7	15.3	0.95
95	7	-0.3	44.4	52.7	2.7	26.2	1.7	15.4	0.95
96	7	0.6	44.4	48.2	2.7	25.5	1.7	14.7	0.95
97	7	0.3	43.8	67.2	2.7	43.2	1.7	27.0	0.95
98	7	-1	45.3	66.9	2.7	26.0	1.7	13.3	0.95
99	7	-0.8	44	66.6	2.7	35.1	1.7	25.7	0.95
100	8	-1.3	43.7	104.1	2.7	41.8	3.3	41.6	1.77
101	8	-0.8	43.7	105.4	2.7	53.6	3.3	49.6	1.77
102	8	-0.3	43.5	126.4	2.7	94.3	3.3	68.9	1.77
103	8	-1.5	43.4	137.5	2.7	51.1	2.8	63.5	1.77
104	8	-1.1	43.3	197.7	2.7	92.1	3.3	95.9	1.77
105	8	-0.6	42.9	211.3	2.7	136.3	3.3	119.7	1.77
106	8	0	42.8	208.2	2.7	173.5	3.3	111.5	1.77
107	8	0.3	43.4	114	2.7	85.8	3.3	58.3	1.77
108	8	0.5	42.8	209.4	2.7	153.0	2.8	96.6	1.77
109	8	0.6	43.1	138.6	2.7	125.7	2.8	79.5	1.77
110	8	1.5	43.1	106.3	2.7	68.9	2.8	42.2	1.77
111	8	1.5	42.7	174	2.7	85.4	2.8	61.4	1.77
112	8	2	43	109.2	2.7	78.4	2.8	43.8	1.77
113	8	2.6	42.8	126	2.7	84.3	2.8	48.9	1.77
114	8	2.5	42.5	145.2	2.7	82.5	2.8	54.4	1.77
115	8	2.9	42.6	133.3	2.7	68.8	2.8	43.8	1.77

ANNEX 4 – Statistical treatment of a comprehensive set of isoseismals observed in France during one century

This Annex consist in a communication that was presented at the 16th European Conference on Earthquake Engineering, copied in the following pages.

From the viewpoint of the present deliverable, a key output of the hereunder communication is that, for any epicentral intensity, all isoseismal radii are log-normally distributed (section 3.1). This feature plays a crucial role in the Annex 5 rationale.

16TH EUROPEAN CONFERENCE ON
EARTHQUAKE ENGINEERING THESSALONIKI
18 - 21 JUNE 2018

STATISTICAL TREATMENT OF A COMPREHENSIVE SET OF ISOSEISMALS OBSERVED IN FRANCE DURING ONE CENTURY

Pierre LABBÉ[1]

ABSTRACT

Isoseismals of the comprehensive set of earthquakes felt in France during a one century period of time are processed in order to derive their statistical features. Considering only epicentral intensities I_0 larger or equal to VI ($I_0 \geq VI$), the set comprises 194 events. It results that, for a given epicentral intensity, radii of isoseismals ($I \geq V$) are log-normally distributed. Intensity attenuation formulas are presented, which give the mean value and the standard deviation of isoseismal radii versus I_0-I, for VIII-IX $\geq I_0 \geq$ VI and $I \geq V$, with most determination coefficients larger than 0.95.

For the purpose of scenarii associated to a given epicentral intensity I_0, formulas are proposed, which provide statistical description of the epicentral isoseismal radius and, associated to it through their correlation coefficient, the rate of isoseismal radius decrease versus I_0-I.

Keywords: Historical seismicity; Isoseismals; Statistics; France

1. INTRODUCTION

For more than 10 years the OECD (OECD 2015) has been recommending that PSHA outputs are tested against instrumental seismicity, historical seismicity and paleoseismicity. In this context the present paper deals with characterization of historical seismicity at the scale of the French territory. The approach is applicable to any territory with a similarly documented historical seismicity.
In order to get a reliable estimate of the historically observed seismic risk at the scale of a territory, it is necessary to get:

a) Statistical data of earthquakes felt in the territory, including their epicentral intensities,
b) For a given epicentral intensity I_0, an evaluation of the isoseismal radii for $I \leq I_0$.

The purpose of this paper is to address point b).

A series of isoseismal maps in the French territory was published by Levret et al. (1994). However it consisted of selected events, not of a compilation of events on a given period of time. In the frame of the SIGMA project (Senfaute 2016), Lambert et al. (2015) processed the comprehensive set of historical earthquakes listed in the SisFrance database (www.sisfrance.net), with epicentral MSK intensities $I_0 \geq$ VI, felt in the French metropolitan territory in the years 1900 to 2007. Macroseismic data of a total of 194 events were gathered and processed, including 82 events with epicenter out of the French territory. The distribution of epicentral intensities is presented in Table 1.

Lambert et al.'s output (2015) consists of an atlas of isoseismal maps, which we process in order to derive empirical intensity attenuation curves. (In the following, intensity values are noticed in Arabic numbers; for instance I=7.5 means VII-VIII intensity.)

[1]Professor, Ecole Spéciale des Travaux Publics, Cachan, France, pierre.labbe@estp.fr, formerly EDF

2 INPUT DATA

In their atlas, Lambert et al. (2015) attach a type to every isoseismal, with the following definitions:

- Type 0: The area of this isoseismal is zero;
- Type 1: The area of the part located in France is known but the total area is unknown;
- Type 2: The total area is known;
- Type 3: The total area is positive but unknown.

For our purpose we select the only isoseismals of type 0 and 2, which results in Table A1 presented in the Appendix. For every of the 194 events, the SisFrance identification number is reported, as well as the date and the name of the event, the epicentral intensity, and the radii of the isoseismals (for instance radii of isoseismals I=6 are reported in the column R6). For practical reasons, we limit our analysis to I≥5. The comprehensive set of isoseismal radii included in Table A1 constitutes our input data. Incidentally it can be noticed that some events (most with epicenter located out of France) do not provide any radius value because of our above mentioned isoseismal Type filter.

Out of Table A1, we designate as 'Class I_0:I' the set of isoseismals I associated to an epicentral intensity I_0. The number of isoseismals per class is indicated in Table 2. For instance the database includes 23 isoseismals I=6 associated to an epicentral intensity I_0=6.5.

Table 1. Number of events per epicentral intensity I_0

I_0	9	8.5	8	7.5	7	6.5	6
Nb of events	1	3	3	15	51	33	88

Table 2. Number of isoseismals per class I_0:I

I_0	9	8.5	8	7.5	7	6.5	6
I=8	0	2	1	Ø	Ø	Ø	Ø
I=7	0	2	2	7	27	Ø	Ø
I=6	0	2	2	5	35	23	62
I=5	0	2	2	6	34	21	69

3 ANALYSIS BY CLASSES

3.1 Statistics

For every class I_0:I, we calculate the mean of the isoseismal radii, and if the number of items in the class is at least five, the standard deviation. Results are presented in Table 3. For instance the class 7:6

Table 3. Mean and standard deviation of radii per class (km)

I_0	8.5	8	7.5	7	6.5	6
			Mean			
I=8	9.10	2.92	Ø	Ø	Ø	Ø
I=7	28.54	13.17	8.52	4.57	Ø	Ø
I=6	69.00	27.74	23.76	13.42	7.06	4.45
I=5	152.83	63.60	58.97	33.92	25.80	15.71
			Standard deviation			
I=8	/	/	Ø	Ø	Ø	Ø
I=7	/	/	6.35	3.77	Ø	Ø
I=6	/	/	17.75	11.00	4.55	4.44
I=5	/	/	42.95	23.63	19.25	13.68

(which consists of 35 isoseismals I=6 associated to an epicentral intensity I_0=7) has a 13.42 km mean radius and an 11.00 km standard deviation.

For classes with at least five items, we test the assumption that the radii are log-normally distributed: For every class we establish the observed standardized repartition of the natural logarithm of the radii in the class (y variable, calculated as per Equation 1) and compare it to the standardized Gaussian repartition. Two example of this comparison are presented in Figure 1, illustrating an excellent fit. Determination coefficients calculated from the series of natural logarithms of observed radii are presented in Table 4, confirming the validity of the assumption.

$$y = (r - \bar{r}) / \sigma_r \quad \text{with } r = \mathrm{Ln}(R) \tag{1}$$

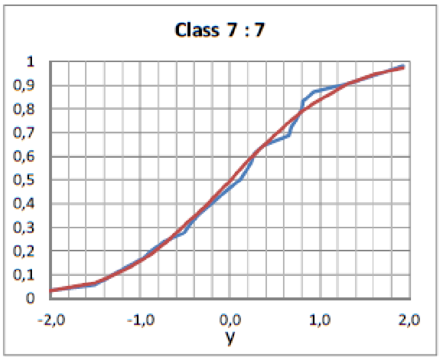

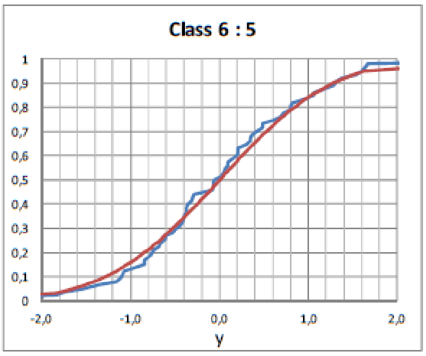

Figure 1. Observed repartition of natural logarithms of radii of isoseismals (blue) compared to the theoretical repartition (red) for two classes of isoseismals.

Table 4. Coefficients of determination for log-normal distributions

I_0	8,5	8	7,5	7	6,5	6
I=8	/	/	Ø	Ø	Ø	Ø
I=7	/	/	0.847	0.990	Ø	Ø
I=6	/	/	0.974	0.965	0.982	0.971
I=5	/	/	0.944	0.956	0.964	0.974

3.2 Intensity attenuation curves

Logarithms of mean, $\overline{R}$, and standard deviation, σ_R, values presented in Table 3 are plotted versus I_0-I in Figure 2. We observe empirical linear relationships represented in the figure by the regression dotted straight lines, corresponding to Equations 2-a and 2-b. As usual for lognormal distributions, we derive the median radius value, R_0, and the dispersion coefficient β_R, which are given by Equations 2-c and 2-d. It is remarkable that β_R is constant (not I_0-I dependant). It comes from the fact that the observed empirical coefficient of variation is constant: COV=$\sigma_R/\overline{R}$ =0.85.

$$\overline{R} = 4.7\, e^{I_0 - I} \quad , \quad \sigma_R = 4\, e^{I_0 - I} \quad , \quad \overline{R} \text{ and } \sigma_R \text{ in km} . \tag{2-a), (2-b}$$

$$R_0 = 3.6\, e^{I_0 - I} \quad , \quad \beta_R = 0.74 \quad , \quad R_0 \text{ in km} . \tag{2-c), (2-d}$$

It is concluded that, in the French seismo-tectonic context, for an event of epicentral intensity I_0 ($I_0 \geq 6$), the isoseismal I radius ($I \geq 5$) appears as a sample of the log-normally distributed random variable characterized by the above Equations 2-a to 2-d.

3

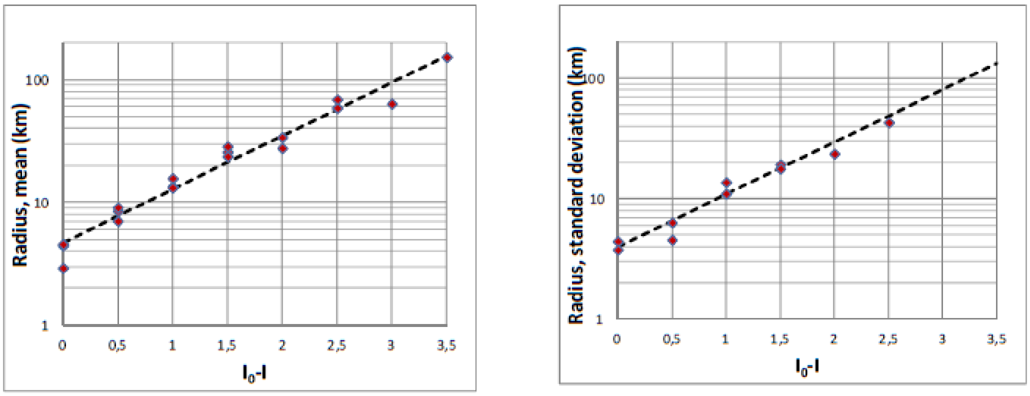

Figure 2. Mean value (left) and standard deviation (right) of isoseismal radii versus I_0-I

This result is very useful to conduct seismic risk analyses at the scale of the French territory. However, it is not sufficient to describe a possible set of isoseismals attached to a given epicentral intensity because in such a scenario, isoseismals cannot be regarded as samples of independent variables.

4 FEATURES OF INDIVIDUAL EARTHQUAKES

In order to analyse the set of isoseismals corresponding to a given event, we select out of Table A1 those 35 events presented in Table A2, which provide at least three isoseismals. For every of them we calculate, in the form of Equation 3, the linear regression between I_0-I and the natural logarithm of the corresponding radius. Four examples of such linear regressions are presented in Figure 3.

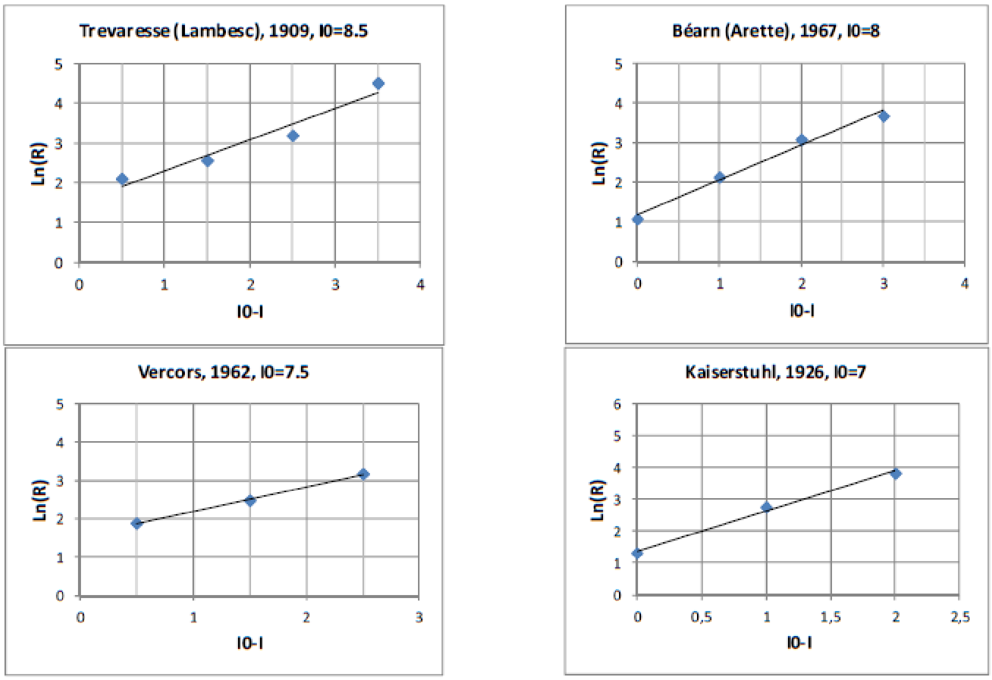

Figure 3. Examples of linear regressions between I_0-I and natural logarithm of radii (km)

$$\mathrm{Ln}(R) = a(I_0 - I) + b \text{ , R in km} \qquad (3)$$

The list of a and b values is included in Table A2. Statistical treatment of a and b shows that a is log-normally while b is normally distributed, with a significant correlation. Numerical values of a and b mean and standard deviation are given in Equation 4, as well as the correlation coefficient, ρ, between Ln(a) and b. The negative value of ρ means that for a given epicentral intensity, the trend is that a faster isoseismal radius decrease is associated to a larger radius of the epicentral area.

$$\bar{a} = 0.95, \quad \sigma_a = 0.27 \quad ; \quad \bar{b} = 1.32, \quad \sigma_b = 0.88 \quad ; \quad \rho(\mathrm{Ln}(a), b) = -0.43 \qquad (4)$$

To simulate a possible set of isoseismal radii ($I \geq 5$) associated to a given epicentral intensity I_0 ($I_0 \geq 6$), it is necessary, first to get a sample of (a, b) according to Equation 4 taking into account that a is log-normally and b normally distributed, and second to apply Equation 3.

Note: It should be noted that, when applied to the subset of Table A2 events, the procedure presented in 3.1 results in slightly different outputs, which reads:

$$\bar{R} = 5.5\, e^{0.9(I_0 - I)} \quad , \quad \sigma_R = 4.2\, e^{0.9(I_0 - I)} \quad , \quad \bar{R} \text{ and } \sigma_R \text{ in km} . \qquad (5\text{-a}), (5\text{-b})$$

Formulas 2 and 5 are corresponding to the same mean value and the same standard deviation for I_0-I =1.5.

5 CONCLUSION AND PERSPECTIVES

On the basis of an atlas of isoseismal maps, encompassing all the events felt in France with intensity equal to or larger than VI during one century, we have derived statistical features of expected isoseismal radii associated to a given epicentral intensity. The method can be used for any territory with a sufficiently documented historical seismicity. It is expected that the output should be similar for territories that are located in a similar sismo-tectonic context.
In order to evaluate the historically observed seismic risk at the scale of the French territory, it is still necessary that a statistical model of expected epicentral intensities be established and that an analysis be carried out, separating areas affected by a given intensity that are located inside the French metropolitan territory from those that are located abroad. This work is in progress.

6. ACKNOWLEDGMENTS

EDF is sincerely acknowledged for having provided the database presented in Table A1.

7. REFERENCES

Lambert J., Monfort-Climent D., Bouc O. (2015) Catalogue of isoseismal areas for 20th century French historical earthquakes ($I_0 \geq 6$). SIGMA-2015-D1-148, internal report. Paper under publication.

Levret A., Backe J.C., Cushing M. (1994). Atlas of macroseismic maps for French earthquakes with their principal characteristics. *Natural Hazards,* 10(1–2): 19–46

OECD (2015), Findings and Recommendations, *Proceedings of the Workshop on Testing Probabilistic Seismic Hazard Analysis Results and the Benefits of Bayesian Techniques*, Pavia, Italy, 4-6 Feb. 2015. NEA/CSNI/R(2015)15. https://www.oecd-nea.org/nsd/docs/2015/csni-r2015-15.pdf

Senfaute G., Pecker A., Labbé P., Sidaner J.-F., Berge-Thierry C., Rzepka J.-P., Contri P. (2016), Contribution of the SIGMA research programme to quantify the uncertainties in seismic hazard assessment, *Proceedings of the 35th General Assembly of the European Seismological Commission*

APPENDIX

Table A1. The 194 events in the Lambert et al. (2015) database and their Type 2 isoseismal radii

Num.	date			Name	I_0	R8	R7	R6	R5
40065	1912	2	9	EMBRUNAIS (ST-ANDRE)	6			1.6	6.3
40067	1913	5	14	MOYENNE-DURANCE (VOLX)	7.5		1.4		
40082	1933	9	19	UBAYE (LE LAUZET)	6.5			2.5	7.4
40092	1949	3	22	UBAYE (LE LAUZET)	6			3.3	9.9
40099	1951	11	30	HAUT-VERDON (CHASTEUIL)	7.5		1.0	5.3	16.2
40109	1959	4	5	UBAYE (ST-PAUL)	7.5		9.7	22.9	40.1
40140	1937	9	30	MOYENNE-DURANCE (LURS)	6			1.2	
40176	1984	6	19	PREALPES DE DIGNE (AIGLUN)	6			2.8	7.5
40203	1997	10	31	PREALPES DE DIGNE (PRADS-HTE-BLEONE)	6				13.5
50032	1904	7	12	BRIANCONNAIS (BRIANCON)	7		3.9	10.7	28.6
50043	1935	3	19	EMBRUNAIS (ST-CLEMENT)	7		12.9	22.8	40.7
50050	1937	12	17	QUEYRAS (GUILLESTRE)	6				14.5
50052	1938	2	15	EMBRUNAIS (CHATEAUROUX)	6				10.4
50057	1938	7	18	QUEYRAS (GUILLESTRE)	7			13.4	30.1
50099	1991	2	11	BRIANCONNAIS (BRIANCON)	6				7.6
110005	1950	6	28	CORBIERES (CAMPLONG-D'AUDE)	6.5			9.8	35.4
120003	1939	5	16	VALLEE DE L'AVEYRON (SEVERAC-LE-CH.)	6			3.6	9.8
130057	1909	6	11	TREVARESSE (LAMBESC)	8.5	8.2	13.0	24.4	91.2
130059	1909	7	10	TREVARESSE (LAMBESC)	6			5.0	22.9
130064	1909	9	22	TREVARESSE (LAMBESC)	6			3.6	14.4
130118	1984	2	19	BASSE-PROVENCE (MIMET)	6			1.1	8.6
160012	1935	9	28	ANGOUMOIS (ROUILLAC)	7		6.6	12.1	30.5
170069	1903	10	27	AUNIS (LA ROCHELLE)	6			2.6	19.5
170077	1958	7	20	ILE D'OLERON	6			1.7	28.7
170079	1972	9	7	ILE D'OLERON	7		6.2	24.2	63.8
180010	1925	9	26	MARCHE-BOISCHAUT (CHATEAUMEIL.-La CHATRE)	6.5			7.8	30.5
200013	1978	4	3	CASTAGNICCIA (CERVIONE)	6			2.2	9.2
230010	1925	12	3	MARCHE-BOISCHAUT (LA CHATRE)	6			5.4	16.6
260097	1901	5	13	BAS-PLATEAUX DAUPHINOIS (MANAS)	7		2.5	8.1	14.9
260120	1934	5	11	TRICASTIN (ROUSSAS)	6			4.3	8.7
260122	1934	5	12	TRICASTIN (VALAURIE)	7		1.0	4.4	7.5
260126	1934	5	16	TRICASTIN (VALAURIE)	6			4.5	10.6
260127	1934	5	16	TRICASTIN (BOUCHET)	6			3.0	10.1
260138	1934	6	24	TRICASTIN (VALAURIE)	6			1.8	4.0
260142	1934	12	9	TRICASTIN (VALAURIE)	6			0.5	2.0
260150	1936	2	13	TRICASTIN (LA GARDE-ADHEMAR)	6			1.5	7.8
260175	1952	6	8	BARONNIES (PIERRELONGUE)	7		0.5	1.1	6.5
290030	1959	1	2	CORNOUAILLE (MELGVEN)	7		7.3	21.2	65.7
300014	1946	9	30	COSTIERE (LE PONT-DU-GARD)	6.5			1.7	6.4
310037	1999	10	4	HAUT-COMMINGES (CIERP)	6			3.1	12.8
380053	1938	12	8	BAS-PLATEAUX DAUPHINOIS (LA SONE)	6			1.5	4.2
380058	1941	8	10	BAS-PLATEAUX DAUPHINOIS (COTE-St-ANDRE)	6			2.6	10.1
380070	1962	4	25	VERCORS (CORRENCON-EN-VERCORS)	7.5		6.6	12.0	23.9
380075	1963	4	25	VERCORS (MONTEYNARD)	7		5.8	10.0	18.6
380080	1963	4	27	VERCORS (MONTEYNARD)	7		1.6	3.9	9.1
380083	1963	12	4	VERCORS (CORRENCON-EN-VERCORS)	6			4.5	8.4

380084	1963	12	7	VERCORS (CORRENCON-EN-VERCORS)	6			3.0	7.5
380085	1963	12	12	VERCORS (CORRENCON-EN-VERCORS)	6			2.1	6.5
380099	1979	11	22	VERCORS (MONTEYNARD)	6			2.1	7.0
390016	1971	6	21	JURA (VAUX-LES-SAINT-CLAUDE)	7		1.5	3.5	5.5
440040	1907	12	12	PAYS DE CHATEAUBRIANT (TREFFIEUX)	6			3.4	15.2
450009	1933	10	3	VAL DE LOIRE (TIGY)	6			3.1	12.2
560019	1902	12	5	ILE DE BELLE-ILE (LE PALAIS)	6			5.5	15.8
560027	1930	1	9	LANDES DE LANVAUX (MEUCON)	7		2.2	9.7	45.6
610009	1927	11	19	BOCAGE NORMAND (FLERS)	6			6.7	30.3
630059	1913	10	16	COMBRAILLE (PIONSAT)	6			3.1	
630069	1957	3	25	LIMAGNE (RANDAN)	6			5.7	12.1
640001	1980	2	29	OSSAU (ARUDY)	7.5		11.1	27.2	49.0
640003	1980	2	29	OSSAU (ARUDY)	6			5.1	34.9
640272	1902	5	6	BEARN (LURBE-SAINT-CHRISTAU)	7		5.9	16.6	63.5
640284	1902	9	8	BEARN (OLORON-SAINTE-MARIE)	7		4.6	11.3	35.7
640292	1911	7	24	BEARN (BENEJACQ-COARRAZE)	7			10.9	42.0
640330	1952	2	7	BEARN (ARETTE)	6			3.4	13.2
640362	1967	8	13	BEARN (ARETTE)	8	2.9	8.4	21.7	39.3
640375	1973	12	13	BEARN (NAY-BOURDETTES)	6.5			4.9	14.2
640385	1977	9	12	PAYS BASQUE (STE-ENGRACE)	6.5			4.7	15.1
640417	1981	2	5	BEARN (NAVARRENX)	6			6.0	12.2
640431	1982	1	6	PAYS BASQUE (ST-JEAN-LE-VIEUX)	6.5			12.0	35.1
640444	1982	8	25	BEARN (S. ARTHEZ-D'ASSON)	6			4.0	12.0
640462	1984	2	25	PAYS BASQUE (BAIGORRY)	6			5.5	15.7
650221	1904	7	13	BIGORRE (BAGNERES-DE-BIGORRE)	7		6.5	28.6	62.8
650244	1905	7	28	BIGORRE (BAGNERES-DE-BIGORRE)	6.5			16.0	33.4
650273	1912	9	15	ARAGON (JACA)	6.5				
650287	1924	2	22	BEARN (S. ARTHEZ-D'ASSON)	7		10.0	17.4	29.9
650324	1930	10	13	LAVEDAN (ARGELES-GAZOST)	6			1.7	6.4
650361	1948	3	16	BIGORRE (CHEUST-JUNCALAS)	6				9.2
650366	1950	1	31	BIGORRE (CAMPAN)	7			14.2	30.8
650374	1952	4	5	LAVEDAN (ARGELES-GAZOST)	6			10.4	21.3
650377	1953	10	13	BIGORRE (CAMPAN)	6			8.8	20.9
650382	1958	11	25	BIGORRE (HECHES)	6.5			7.0	30.3
650500	2002	5	16	LAVEDAN (AUCUN)	6			1.3	8.2
650505	2006	11	17	BIGORRE (GAZOST)	6			6.6	18.5
660061	1920	11	28	FENOUILLEDES (ST-PAUL-DE-FENOUILLET)	7		2.7	6.4	27.1
660068	1922	9	23	FENOUILLEDES (ST-PAUL-DE-FENOUILLET)	6.5			5.9	21.9
660073	1922	12	28	PLAINE DU ROUSSILLON (MILLAS)	6			7.6	13.4
660095	1996	2	18	FENOUILLEDES (ST-PAUL-DE-FENOUILLET)	6			7.8	20.0
670096	1952	9	29	OUTRE-FORET (WISSEMBOURG)	6.5			5.2	
670102	1952	10	8	OUTRE-FORET (WISSEMBOURG)	6.5			9.2	
670106	1959	9	4	PLAINE DE BASSE-ALSACE (ERSTEIN)	6			3.6	9.8
680065	1901	5	22	PLAINE DE HAUTE-ALSACE (ST-LOUIS)	6			3.0	14.0
680091	1980	7	15	PLAINE DE HAUTE-ALSACE (HABSHEIM)	6.5			5.2	26.3
700013	1955	11	3	AVANT-PAYS JURAS. (MONTARLOT-LES-RIOZ)	6			1.1	5.4
700017	1955	11	23	AVANT-PAYS JURAS. (MONTARLOT-LES-RIOZ)	6			2.7	8.0
730165	1947	5	27	LAC DU BOURGET (JONGIEUX)	6			1.2	6.1
730174	1958	3	30	LAC DU BOURGET (CONJUX)	6.5			5.9	14.2
730177	1958	9	15	BUGEY (LA BALME-DE-SILLINGY)	6			1.5	4.8
740060	1905	4	29	MASSIF DU MONT-BLANC (LAC D'EMOSSON)	7.5		19.4	51.4	114.8

740067	1905	8	13	MASSIF DU MONT-BLANC (CHAMONIX)	7			13.0	
740069	1909	2	17	CHABLAIS (ABONDANCE)	6			2.9	10.5
740079	1936	4	17	AVANT-PAYS SAVOYARD (FRANGY)	7			3.7	10.6
740094	1968	6	27	CHABLAIS (ABONDANCE)	6.5			2.6	5.1
740097	1968	8	19	CHABLAIS (ABONDANCE)	7		2.4	8.7	31.9
740119	1980	12	2	BAUGES (FAVERGES)	6.5			3.7	16.0
740150	1994	12	14	GENEVOIS (LES VILLARDS-SUR-THONES)	6			5.8	20.9
740153	1996	7	15	AV. PAYS SAVOYARD (EPAGNY-ANNECY)	7		1.8	8.8	23.0
830006	1932	5	1	MEDITERRANEE (S. MARSEILLE)	6				
840066	1905	4	10	BARONNIES (VAISON-LA-ROMAINE)	7		1.1	3.5	15.3
840068	1924	9	24	COMTAT (CADEROUSSE)	6.5			1.4	4.0
840074	1927	7	24	BARONNIES (MALAUCENE)	7		1.3	3.6	7.7
860021	1901	11	18	BRANDES DU HAUT-POITOU (CHARROUX)	6			6.6	24.9
880053	1984	12	29	HAUTES-VOSGES (ELOYES-REMIREMONT)	6			5.8	16.1
880077	2003	2	22	PAYS FORESTIER SOUS-VOSGIEN (RAMBERV.)	6.5			11.4	32.9
1100014	1938	6	11	FLANDRES (RENAIX-OUDENAARDE)	7		16.7	56.5	87.8
1100022	1983	11	8	PAYS DE LIEGE (LIEGE)	7.5				
1100079	1965	12	15	HAINAUT (MAURAGE)	7		3.0	4.4	9.1
1100083	1966	1	16	HAINAUT (CARNIERES)	7		3.3	7.1	10.6
1100110	1992	4	13	LIMBOURG (ROERMOND)	6.5				
1100119	1928	1	14	HAUTES-FAGNES (VERVIERS)	6			3.6	13.1
1110017	1926	6	28	VALLEE DU RHIN (KAISERSTUHL)	7		3.7	15.8	45.4
1110019	1957	8	29	JURA SOUABE (TAILFINGEN)	6			6.1	
1110021	1965	9	19	FORET NOIRE (ST-BLASIEN)	6			4.2	26.9
1110022	1974	5	21	FORET NOIRE (WEHR)	6			2.5	
1110059	1903	3	22	VALLEE DU RHIN (KARLSRUHE)	6.5			5.5	10.1
1110061	1911	11	16	JURA SOUABE (EBINGEN)	8.5	10.0	44.1	113.6	214.4
1110062	1913	7	20	JURA SOUABE (TUBINGEN)	6			34.1	105.6
1110063	1915	6	2	JURA FRANCONIEN (INGOLSTADT)	7				
1110065	1924	12	11	JURA SOUABE (EBINGEN)	6.5			11.5	
1110066	1924	12	12	JURA SOUABE (EBINGEN)	6.5				
1110068	1930	10	7	ALPES BAVAROISES (NAMLOS)	7				
1110069	1933	2	8	VALLEE DU RHIN (RASTATT)	7		4.2	15.6	36.4
1110070	1933	2	21	JURA SOUABE (PFEFFINGEN)	6				
1110074	1935	6	27	JURA SOUABE (KAPPEL)	7.5				
1110075	1935	12	30	VALLEE DU RHIN (OFFENBURG)	6				
1110076	1935	12	30	VALLEE DU RHIN (OFFENBURG)	7			16.6	67.9
1110077	1943	5	2	JURA SOUABE (EBINGEN)	7				
1110078	1943	5	28	JURA SOUABE (BALINGEN)	7				
1110079	1947	4	14	JURA SOUABE (EBINGEN)	6				
1110080	1947	6	28	JURA SOUABE (ONSMETTINGEN)	6.5				
1110083	1948	6	7	VALLEE DU RHIN (KARLSRUHE)	7				
1110085	1952	2	24	VALLEE DU RHIN (LUDWIGSHAFEN)	6.5			19.4	65.7
1110086	1969	2	26	JURA SOUABE (TAILFINGEN)	7				
1110087	1970	1	22	JURA SOUABE (ONSMETTINGEN)	7				
1110091	1978	9	3	JURA SOUABE (ONSMETTINGEN)	7.5				
1110096	1951	3	14	HAUTES-FAGNES (EUSKIRCHEN)	7.5				
1110221	2004	12	5	BADEN-WURTTEMBERG (WALDKIRCH)	6				
1120023	1924	4	15	VALAIS (VISP)	7				
1120028	1946	1	25	VALAIS (CHALAIS)	7.5		10.5		
1120031	1946	1	26	VALAIS (CHALAIS)	7				

8

1120033	1946	5	30	VALAIS (CHALAIS)	7			
1120035	1954	5	19	VALAIS (N-W. SION)	7			
1120037	1954	7	29	VALAIS (MONTANA)	6.5			
1120038	1960	3	23	VALAIS (BRIG)	7			
1120044	1925	1	8	JURA SUISSE (ORBE-LIGNEROLLE)	6.5		6.1	61.4
1120077	1910	5	26	JURA SUISSE (LAUFEN)	6		8.8	35.5
1120078	1964	3	14	UNTERWALD (SARNEN)	7			
1120086	1929	3	1	PLATEAU SUISSE (YVERDON)	6.5			
1120109	1984	9	5	ZURICH	6			
1120261	1915	8	25	BAS-VALAIS (MARTIGNY)	6.5			
1120271	1933	8	12	PLATEAU SUISSE (MOUDON)	6.5			
1130067	1905	5	30	PIEMONT (FOSSANO)	6			24.7
1130068	1906	8	11	RIVIERA DI PONENTE (TAGGIA)	6			14.3
1130070	1920	9	7	TOSCANE (FIVIZZANO)	9			
1130078	1936	12	11	PIEMONT (PIGNA)	6			9.6
1130082	1958	5	4	PIEMONT (VALDIERI)	6		9.4	36.3
1130085	1963	7	19	MEDITERRANEE (S. IMPERIA)	7			
1130086	1963	7	19	MEDITERRANEE (S. IMPERIA)	7.5			109.9
1130088	1963	7	27	MEDITERRANEE (S. IMPERIA)	7.5			
1130091	1966	4	7	PIEMONT (ENTRACQUE)	6.5		3.2	10.3
1130092	1968	4	18	RIVIERA DI PONENTE (DIANO MARINA)	6		4.5	10.0
1130098	1972	1	18	RIVIERA DI PONENTE (PIETRA LIGURE)	6		3.9	17.2
1130101	1976	5	6	FRIOUL (UDINE)	8.5			
1130104	1941	2	23	PIEMONT (PRAZZO)	6			
1130107	1955	5	12	PIEMONT (STROPPO)	7		11.1	24.2
1130108	1955	6	20	PIEMONT (PRAZZO)	7			
1130121	1914	10	26	PIEMONT (SACRA DI SAN MICHELE)	7		40.1	95.6
1130122	1947	2	17	PIEMONT (PRAZZO)	7.5			
1130129	1927	12	11	PIEMONT (SUSA)	6			17.2
1130131	1968	6	18	VAL D'AOSTE (ARNAZ)	6.5			
1130132	1901	10	30	LOMBARDIE (W. BRESCIA)	8			
1130133	1948	11	13	SARDAIGNE	6			
1130135	1980	1	5	PIEMONT (PINEROLO)	7	4.1	10.6	28.6
1130146	1981	4	22	MEDITERRANEE (S. SAN REMO)	6			
1130214	1918	1	13	LOMBARDIE (MILANO)	6			
1130362	1938	12	23	CANAVESE (LOCANA)	6			
1130560	1995	4	21	RIVIERA DI PONENTE (VINTIMILLE)	6			
1140018	1903	4	20	CATALOGNE (ROSAS)	6			
1140020	1927	3	12	CATALOGNE (MONTSENY)	6			
1140024	1923	11	19	VAL D'ARAN (VIELLA)	8	18.0	33.8	87.8
1140026	1924	2	27	VAL D'ARAN (VIELLA)	6			28.6
1140046	1919	11	29	VAL D'ARAN (BOHI)	6			33.2
1140048	1923	7	10	NAVARRE (BERDUN)	7.5			
1140126	2004	9	21	CERDAGNE	6			
1150008	1931	6	7	MER DU NORD (DOGGER BANK)	7			
1150020	1926	7	30	JERSEY	6.5			66.1

Table A2. Events with at least three isoseismals, and associated linear regressions

Num.	I_0	R8	R7	R6	R5	a	b
130057	8.5	8.2	13.0	24.4	91.2	0.79	1.52
1110061	8.5	10.0	44.1	113.6	214.4	1.01	2.02
640362	8	2.9	8.4	21.7	39.3	0.88	1.17
1140024	8		18.0	33.8	87.8	0.79	2.04
40099	7.5		1.0	5.3	16.2	1.40	-0.63
40109	7.5		9.7	22.9	40.1	0.71	1.97
380070	7.5		6.6	12.0	23.9	0.64	1.55
640001	7.5		11.1	27.2	49.0	0.74	2.09
740060	7.5		19.4	51.4	114.8	0.89	2.55
50032	7		3.9	10.7	28.6	1.00	1.37
50043	7		12.9	22.8	40.7	0.57	2.56
160012	7		6.6	12.1	30.5	0.77	1.83
170079	7		6.2	24.2	63.8	1.16	1.89
260097	7		2.5	8.1	14.9	0.89	1.02
260122	7		1.0	4.4	7.5	1.02	0.14
260175	7		0.5	1.1	6.5	1.31	-0.90
290030	7		7.3	21.2	65.7	1.10	1.97
380075	7		5.8	10.0	18.6	0.58	1.74
380080	7		1.6	3.9	9.1	0.86	0.49
390016	7		1.5	3.5	5.5	0.65	0.47
560027	7		2.2	9.7	45.6	1.51	0.78
640272	7		5.9	16.6	63.5	1.19	1.73
640284	7		4.6	11.3	35.7	1.02	1.49
650221	7		6.5	28.6	62.8	1.13	1.99
650287	7		10.0	17.4	29.9	0.55	2.30
660061	7		2.7	6.4	27.1	1.14	0.91
740097	7		2.4	8.7	31.9	1.30	0.86
740153	7		1.8	8.8	23.0	1.26	0.71
840066	7		1.1	3.5	15.3	1.31	0.05
840074	7		1.3	3.6	7.7	0.90	0.30
1100014	7		16.7	56.5	87.8	0.83	2.95
1100079	7		3.0	4.4	9.1	0.55	1.05
1100083	7		3.3	7.1	10.6	0.58	1.25
1110017	7		3.7	15.8	45.4	1.25	1.38
1110069	7		4.2	15.6	36.4	1.08	1.52

ANNEX 5 – Possible effect of extreme historical events on the outputs of the study

1 Introduction

Some historical events that occurred before 1905 were documented by Levret et al. (1994) in terms of isoseismal diameters, and a few other ones by Lambert et al. (1997). The most significant of them by the size of isoseismals are summarized in Table A5-1. For instance, isoseismals of the Détroit de Calais earthquakes (I_0=7,5) are much larger than the largest in the 1900-2007 database, which are R7 = 19.4 km, R6 = 51.4 km and R5 = 114.8 km, these three values being due to the Massif du Mont Blanc earthquake (Lac d'Emosson), dated 29 April 1905 (event 740060 in Annex 4).

Table A5-1 Outstanding historical earthquakes

Name	Date	I_0	R9	R8	R7	R6	R5
Bâle	18/10/1356	9		30			
Détroit de Calais	06/04/1580	7.5			30	111	208
Bigorre	21/06/1660	8.5		16	44	113	240
Bouin	25/01/1799	7.5			18	100	180
Brenne	14/09/1866	7			15	32	170
Vallée de la Saône	24/06/1878	6.5				30	52
Limagne	26/08/1892	6.5				45	75

A consequence of this situation is that we should wonder whether the seismic hazard assessment that we have carried out could result in different outputs in case we account for these large events. We are going first to present the rationale on the case of the Détroit de Calais earthquake. Then we shall present results obtained for the other earthquakes introduced in Table A5-1.

2 Rationale

As the Detroit de Calais earthquake occurred in 1580, an ideal way to answer the above question would be that we have at our disposal the comprehensive series of isoseismals for all the I_0=7,5 earthquakes that occurred, say as of the early 1500's. As we observed 15 such events on 1900-2007, it means that we would ideally handle approximately 75 events since 1500.

This is not such a large number of events and we could think of launching a research on them. However, it is very probable that we would face a completeness issue because, in the population of I_0=7.5 earthquakes, some of them are of small extension (e.g. event 40099 in Annex 4) and the track of such events in the 16th or 17th century may be lost. On the opposite we may assume that earthquakes with a large extension are obviously better documented and that we do not miss the largest ones in the databases.

Consequently, we are led to raise the following question: Considering the population of I_0=7.5 earthquakes, such as characterised by its statistics on the 1900-2007 period of time (presented in Annex 4), is it likely that its largest event on the last four and a half centuries be represented by the Détroit de Calais earthquake?

In order to answer this question, we found the rationale on

- The statistics of classes of isoseismals I_0:I introduced in Annex 4, in particular on the fact that isoseismal radii can be regarded as log-normally distributed random variables.
- The mathematics of extremes, which predict the distribution of the maximum in a set of n samples of such a random variable.

3 Mathematical background on extreme values of random variables

For the sake of clarity and simplicity, we are reasoning on the case of log-normally distributed variables that pertain to our case.

Let's consider a random variable x, entirely characterized by its mean value m and standard deviation σ. We pick at random n samples of x and we retain the maximum, X. We may pick again n other samples and obtain another maximum. It means that X appears as a new random variable. It is clear that, would we multiply x by λ, X would also be multiplied by λ. Consequently, we may limit ourselves to considering the random variables y=x/m (of mean value 1 and standard deviation s=σ/m) and Y=X/m. It is clear that the distribution of Y is depending on s and n.

Distributions of extremes were studied by several authors, in particular by Fréchet, Gumbel and Weibull, whose name were given to 3 different possible distributions of Y (actually there are only 3 possible types). For a log-normally distributed y random variable, its maximum is asymptotically distributed according to the Gumbel distribution. Asymptotically means that Y distribution trends towards a Gumbel type for large values of n. However, this convergence is slow and the Gumble formula is not valid for small values of n as those we may encounter when dealing with historical seismicity. Therefore, we use tables of values that provide the mean value of Y (Table A5-2) and its standard deviation (Table A5-3) versus s and n.

Table A5-2. Mean values of Y versus s and n

s\n	5	10	15	20	30	50	100	200	500	1000
0.1	1.12	1.162	1.185	1.2	1.221	1.247	1.279	1.31	1.348	1.376
0.2	1.246	1.339	1.391	1.427	1.477	1.537	1.617	1.695	1.794	1.868
0.3	1.374	1.528	1.616	1.678	1.764	1.871	2.016	2.16	2.35	2.494
0.4	1.504	1.725	1.855	1.947	2.079	2.245	2.475	2.708	3.023	3.268
0.5	1.631	1.926	2.103	2.232	2.416	2.654	2.988	3.335	3.815	4.196
0.6	1.755	2.128	2.357	2.525	2.77	3.091	3.549	4.035	4.723	5.279
0.7	1.874	2.327	2.613	2.824	3.135	3.549	4.151	4.801	5.739	6.512
0.8	1.988	2.523	2.866	3.123	3.506	4.022	4.784	5.622	6.854	7.887
0.9	2.095	2.712	3.115	3.42	3.878	4.503	5.441	6.489	8.056	9.39
1	2.195	2.894	3.358	3.712	4.248	4.988	6.114	7.391	9.331	11.007
1.1	2.29	3.068	3.592	3.996	4.613	5.473	6.797	8.319	10.667	12.724
1.2	2.378	3.235	3.819	4.272	4.97	5.953	7.484	9.267	12.053	14.525
1.3	2.46	3.393	4.036	4.54	5.319	6.427	8.171	10.225	13.478	16.397
1.4	2.537	3.543	4.244	4.797	5.659	6.892	8.854	11.19	14.933	18.328
1.5	2.609	3.685	4.444	5.045	5.987	7.347	9.531	12.156	16.408	20.306

Table A5-3. Standard deviation of Y versus s and n

s\n	5	10	15	20	30	50	100	200	500	1000
0.1	0.076	0.069	0.066	0.064	0.061	0.059	0.056	0.053	0.051	0.049
0.2	0.169	0.16	0.156	0.153	0.149	0.146	0.142	0.139	0.136	0.134
0.3	0.281	0.275	0.273	0.271	0.269	0.268	0.267	0.266	0.268	0.269
0.4	0.411	0.415	0.418	0.42	0.424	0.429	0.437	0.446	0.459	0.47
0.5	0.558	0.58	0.593	0.602	0.616	0.634	0.659	0.686	0.723	0.753
0.6	0.72	0.768	0.796	0.816	0.845	0.883	0.936	0.991	1.069	1.131
0.7	0.895	0.977	1.026	1.061	1.111	1.177	1.27	1.368	1.505	1.615
0.8	1.081	1.205	1.28	1.334	1.412	1.515	1.661	1.816	2.036	2.214
0.9	1.277	1.45	1.556	1.633	1.746	1.894	2.107	2.336	2.664	2.933
1	1.48	1.71	1.851	1.956	2.109	2.311	2.606	2.926	3.39	3.775
1.1	1.69	1.981	2.164	2.299	2.498	2.764	3.155	3.583	4.212	4.739
1.2	1.905	2.263	2.49	2.659	2.91	3.248	3.75	4.304	5.126	5.823
1.3	2.124	2.554	2.829	3.036	3.344	3.761	4.386	5.084	6.13	7.024
1.4	2.347	2.852	3.179	3.425	3.795	4.3	5.061	5.919	7.217	8.338
1.5	2.572	3.156	3.537	3.826	4.262	4.861	5.771	6.805	8.384	9.758

4 Application to an example

Lets consider as an example the class of isoseismals I_0=7,5:I=6 and the Détroit de Calais earthquake.

For I_0=7,5:I=6 , the Annex 4 Formula (2) provides:

- m = 21.1 km and σ = 17.9 km, corresponding to s=0.85.

Taking into account that 15 events I_0=7.5 were observed on 1900-2007 (see Annex 4), we may expect approximately n = 65 such events on a four and a half centuries period of time. Interpolating in the Tables A5-2 and A5-3 for s=0.85 and n=65 leads to:

- Y mean = 4.56.
- Y standard deviation= 1.77.

For m = 21.1 km, we derive:

- X mean = 4.56 x 21.1 = 96 km
- X mean + standard deviation= (4.56 + 1.77) x 21.1 = 133 km.

The observed radius of the isoseismal I=6 of the Détroit de Calais earthquake is R6 = 111 km (See Table A5-1). It lies between the mean value, 95.4 km, and the mean plus one standard deviation, 133 km, of the expected maximum value of R6 on four and a half centuries.

5 Outputs and conclusion

Calculation outputs for R5, R6 an R7 of Détroit de Calais earthquake versus the expected maximum values are summarized in the Table A5-4, as well as similar outputs for the 7 events presented in Table A5-1. In this table, Ns is number of centuries considered for calculating features of the expected maximum isoseismal radii. Except for the Détroit de Calais event (as indicated above), Ns is calculated on the basis of the completion dates provided by Secanell et al. (2007), presented in Table A5-5:

Table A5-4 Comparison of radii of historical isoseismals with expected maximum values

Name	Date	I_0	Ns	R8	R7	R6	R5
Bâle	18/10/1356	9	7.2	**30**/29/16			
Détroit de Calais	06/04/1580	7.5	4.5		**30**/35/14	**111**/96/37	**208**/261/101
Bigorre	21/06/1660	8.5	5.2	**16**/23/11	**44**/62/30	**113**/169/81	**240**/461/219
Bouin	25/01/1799	7.5	2.7		**18**/31/13	**100**/83/34	**180**/224/93
Brenne	14/09/1866	7	2.7		**15**/25/9	**32**/69/25	**170**/187/67
Vallée de la Saône	24/06/1878	6.5	1.7			**30**/33/13	**52**/91/36
Limagne	26/08/1892	6.5	1.7			**45**/33/13	**75**/91/36
Ns: Number of centuries considered for calculating features of the expected maximum isoseismal radii. **hh**/mm/ss: **historicaly observed value** / expected maximum-mean / expected maximum-standard deviation							

Table A5-5 Completeness dates of historical earthquakes in France (excerpt from Lambert et al. 1996)

Zone	intensités IV et IV-V	intensités V et V-VI	intensités VI et VI-VII	intensités VII et VII-VIII	intensités VIII et VIII-IX	intensités IX et IX-X
France	1920	1880	1850	1750	1500	1300

Even though some radii look very large, it can be observed that they are generally below the expected maximum value, four of them are larger than the mean expected maximum but none of them exceeds the mean plus one standard deviation.

In other words, taking the example of the Brenne earthquake, would we simulate a series of 2.7 centuries of events with epicentral intensity I_0=7 and characterized by the 1900-2007 observations, we would obtain a series of extreme events that would cover the Brenne earthquake. And similarly for the other events.

In conclusion, the analysis of large historical events in the light of the statistical model of isoseismals resulting from the 1900-2007 database do not lead to the conclusion that the hazard calculated on the basis of this database should be amended in order to take into account those large events.

ANNEX 6 – Effect of fragility curves choice on seismic risk results

This annex shows the difference between the seismic risks according to the fragility curve that is used.

The fragility curves used in this study are determined by the approach of Lagomarsino & Cattari (2014) with two conversion relations (Murphy & O'Brien (1977) and Faccioli & Cauzzi (2006)).

Two others fragility curves, as indicated in the hereunder table A6-1, are here used to calculate the seismic risk of the continental France in order to analyse the impact of a fragility curve change.

Table A6-1: Alternative fragility data

	Milutinovic et al. (2003)		Rota et al. (2010)	
Damage grade	a_D	β_D	a_D	β_D
D=2	1.76 ms^{-2}	0.50	1.97 ms^{-2}	0.29
D=3	2.83 ms^{-2}	0.55	2.68 ms^{-2}	0.29

Impacts are not significant as presented in the hereunder pictures for damages 2 and 3.